**Texas A&M
Transportation
Institute**

# Enhancing Freeway Safety Prediction Models: Technical Report

## Technical Report 0-7067-R1

Cooperative Research Program

| 1. Report No.<br>FHWA/TX-22/0-7067-R1 | 2. Government Accession No. | 3. Recipient's Catalog No. |
|---|---|---|
| 4. Title and Subtitle<br>ENHANCING FREEWAY SAFETY PREDICTION MODELS: TECHNICAL REPORT | | 5. Report Date<br>Published: September 2023 |
| | | 6. Performing Organization Code |
| 7. Author(s)<br>Michael P. Pratt, Srinivas R. Geedipally, Minh Le, Lingtao Wu, Raul Avelar, Subasish Das, and Dominique Lord | | 8. Performing Organization Report No.<br>Report 0-7067-R1 |
| 9. Performing Organization Name and Address<br>Texas A&M Transportation Institute<br>The Texas A&M University System<br>College Station, Texas 77843-3135 | | 10. Work Unit No. (TRAIS) |
| | | 11. Contract or Grant No.<br>Project 0-7067 |
| 12. Sponsoring Agency Name and Address<br>Texas Department of Transportation<br>Research and Technology Implementation Office<br>125 E. 11th Street<br>Austin, Texas 78701-2483 | | 13. Type of Report and Period Covered<br>Technical Report:<br>January 2020–June 2022 |
| | | 14. Sponsoring Agency Code |

16. Abstract

Safety prediction models have been developed for urban freeway segments in Texas and elsewhere to apply to cross sections up to 10 lanes wide. These models are documented resources such as TxDOT's *Roadway Safety Design Workbook* and the *Highway Safety Manual* and applied in several spreadsheet-based analysis tools. These tools are acknowledged in the *Project Development Process Manual* and have been used by various district personnel, particularly in the evaluation of project alternatives or analysis of design exceptions. However, additional research is needed to address knowledge gaps as well as to develop updated local calibration factors for the models. Specifically, safety prediction models do not exist for 12-lane freeway segments or freeway segments with managed lanes (e.g., high-occupancy-vehicle or high-occupancy-toll lanes).

The research team derived local calibration factors for models for urban freeway segments with 4–10 lanes, assessed the applicability of the 10-lane urban freeway model to freeway segments with 11 or more lanes, and developed new safety prediction models for segments with managed lanes. The research team also developed an analysis tool to help practitioners implement the new models to facilitate analysis of complex urban freeway configurations, such as cases where an urban freeway widening project requires challenging tradeoffs between narrowing lanes or inside or outside shoulders.

| 17. Key Words<br>Highway Safety, Highway Design, Safety Management, Geometric Design | 18. Distribution Statement<br>No restrictions. This document is available to the public through NTIS:<br>National Technical Information Service<br>Alexandria, Virginia 22312<br>http://www.ntis.gov | | |
|---|---|---|---|
| 19. Security Classif. (of this report)<br>Unclassified | 20. Security Classif. (of this page)<br>Unclassified | 21. No. of Pages<br>70 | 22. Price |

**Form DOT F 1700.7 (8-72) Reproduction of completed page authorized**

# ENHANCING FREEWAY SAFETY PREDICTION MODELS: TECHNICAL REPORT

by

Michael P. Pratt, P.E.
Assistant Research Engineer

Raul Avelar, Ph.D.
Research Scientist

Srinivas R. Geedipally, Ph.D., P.E.
Research Engineer

Subasish Das, Ph.D.
Associate Research Scientist

Minh Le, P.E.
Associate Research Engineer

Texas A&M Transportation Institute

Lingtao Wu, Ph.D., P.E.
Associate Research Engineer

and

Dominique Lord, Ph.D.
Professor
Texas A&M University

# DISCLAIMER

This research was performed in cooperation with the Texas Department of Transportation (TxDOT) and the Federal Highway Administration (FHWA). The contents of this report reflect the views of the authors, who are responsible for the facts and the accuracy of the data published herein. The contents do not necessarily reflect the official view or policies of FHWA or TxDOT. This report does not constitute a standard, specification, or regulation. It is not intended for construction, bidding, or permitting purposes. The engineer in charge of the project was Michael P. Pratt, P.E. #102332.

The United States Government and the State of Texas do not endorse products or manufacturers. Trade or manufacturers' names appear herein solely because they are considered essential to the object of this report.

# ACKNOWLEDGEMENTS

# TABLE OF CONTENTS

# LIST OF FIGURES

# LIST OF TABLES

# CHAPTER 1: OVERVIEW

## INTRODUCTION

Several research projects on freeway safety performance have been sponsored by Texas, other states, and federal agencies over the past 15 years. These research projects have yielded resources like the *Roadway Safety Design Workbook* (*1*) and chapters for the *Highway Safety Manual* (HSM) (*2*), among others. Safety prediction models in these resources can be used to estimate the crash frequency for a freeway segment of interest as a function of key site variables. However, due to the passage of time since the 2009 publication of the *Roadway Safety Design Workbook* and the fact that the HSM freeway models were calibrated using data from other states, there is a need to re-evaluate and re-calibrate safety prediction models for freeways in Texas.

Safety analysis is becoming increasingly important for projects involving widening or realigning urban freeways, since these projects are often complex and require tradeoffs with key geometric design variables. For example, the addition of lanes may require accepting a narrower lane width or narrower shoulders, since the cost of acquiring right-of-way for widening projects in urban areas is usually significant. Additionally, a growing number of urban freeway improvement projects are involving widening to more than 10 general-purpose lanes or construction of new managed-lane facilities such as high-occupancy vehicle (HOV) or toll lanes. No safety prediction models exist for freeway segments with more than 10 lanes, nor for managed-lane facilities if the analyst needs to estimate the crash frequency in the managed lanes and the adjacent general-purpose lanes separately.

## RESEARCH APPROACH

The research team built a database of urban freeway segments in Texas and used the database to calibrate the urban freeway models in the HSM. The research team applied a three-stage process to compute local calibration factors for the HSM models and assessed the goodness of fit of the calibrated models. These calibrated models allow practitioners to consider a wide range of site characteristics, including traffic volume; cross-sectional widths; longitudinal barrier presence; rumble strip presence; and location, type, and volume of upstream and downstream ramp entrances and exits. Some of these variables were not included in earlier safety prediction models that were developed for Texas. The research team also assessed the models' applicability to urban freeway segments with 12 general-purpose lanes and determined that the 10-lane model from the HSM can be extended to these wider segments with an appropriate set of derived calibration factors. Finally, the research team conducted a detailed review of crash reports from crashes that occurred on urban freeways with managed lanes, allocated the crashes to either the managed lanes or the adjacent general-purpose lanes, and developed new safety prediction models specifically for the managed lanes. These new models account for variables such as traffic volume, cross-sectional widths, buffer type (i.e., pavement stripe, pylons, or concrete buffer), and location and design of access points.

# CHAPTER 2: LITERATURE REVIEW

## INTRODUCTION

Safety prediction models have been developed for urban freeway segments in Texas and elsewhere to apply to cross sections up to 10 lanes wide. These models are documented in resources such as the Texas Department of Transportation's (TxDOT's) *Roadway Safety Design Workbook* (*1*) and the HSM (*2, 3*) and are applied in several spreadsheet-based analysis tools that accompany these documents. These tools are acknowledged in TxDOT's *Project Development Process Manual* (*4*) and have been used by various district personnel, particularly in the evaluation of project alternatives or analysis of design exceptions. However, additional research is needed to address knowledge gaps as well as to develop updated local calibration factors for the models. Specifically, safety prediction models do not exist for freeway segments with 11 or more lanes or freeway segments with managed lanes (e.g., high-occupancy-vehicle or high-occupancy-toll lanes).

This chapter describes a literature review that summarizes freeway safety prediction models that have been developed for urban freeway facilities in the past two decades. The scope is limited to urban facilities because the facilities of interest (i.e., freeways with 11 or more lanes or freeways with managed lanes) do not exist in rural areas. This chapter is divided into two parts. The first part discusses and compares freeway safety prediction models from the literature. The second part summarizes issues and insights with statistical modeling methods used to calibrate safety prediction models.

## SAFETY PREDICTION MODELS

Freeways have been the subject of safety analysis research projects over the past 20 years in Texas and elsewhere. These projects include TxDOT Research Project 0-4703 (*1*), TxDOT Research Project 0-6811 (*5*), Federal Highway Administration (FHWA) Task Order T-5012 (*6*), and National Cooperative Highway Research Program (NCHRP) Project 17-45 (*3*). Most of these projects have focused on freeway facilities that are more abundant in terms of centerline mileage. Relatively little research has been conducted on freeway segments with 11 or more lanes or freeways with managed lanes because of their relative rarity. However, because of significant and growing demand for freeway capacity in urbanized areas, such facilities are becoming more common and are often constructed in corridors with limited right-of-way. As a result, wider freeways sometimes have lanes and shoulders that are narrower than desired, and design tradeoffs have to be made between narrowing the different cross-sectional elements, especially in constrained locations like between bridge columns.

Safety analysis is performed in various stages of the project development process, including project identification, alternatives analysis, preliminary design, and final design (*4*). It is particularly common for safety analysis to be conducted as part of the design exception process. These efforts require knowledge of safety trends. The current state of this knowledge is summarized in the following sections.

**Highway Safety Manual Models**

  Chapters 18 and 19 of the HSM contain safety performance functions (SPFs) for freeway mainline segments and ramps, respectively (*2*).  These models were calibrated using data from the states of Washington, California, and Maine (*3*).  Equations 1–5 describe the models for urban freeway mainline segments with no ramp entrances or exits present.  These equations provide separate estimates for multiple-vehicle and single-vehicle crashes, as well as for fatal-and-injury (FI) and property-damage-only (PDO) crashes.  Table 1 provides the calibration coefficients for Equations 2–5.  Note that Equation 1 provides the base crash frequency, which is the crash frequency for a segment that has geometric and traffic control characteristics that match the "base" or "typical" conditions identified in the analysis of the model calibration dataset.  The HSM also provides crash modification factors (CMFs) for Equations 2–5 that allow the analyst to adjust for conditions that differ from the base conditions.

$$N = N_{MV,FI} + N_{MV,PDO} + N_{SV,FI} + N_{SV,PDO} \qquad (1)$$

with:

$$N_{MV,FI} = L \times b_{n,MV,FI} \times \left(\frac{AADT}{1000}\right)^{1.492} \qquad (2)$$

$$N_{MV,PDO} = L \times b_{n,MV,PDO} \times \left(\frac{AADT}{1000}\right)^{1.936} \qquad (3)$$

$$N_{SV,FI} = L \times b_{n,SV,FI} \times \left(\frac{AADT}{1000}\right)^{0.646} \qquad (4)$$

$$N_{SV,PDO} = L \times b_{n,SV,PDO} \times \left(\frac{AADT}{1000}\right)^{0.876} \qquad (5)$$

where:

$N$ = base number of crashes per year;
$N_{MV,FI}$ = number of multiple-vehicle FI crashes per year;
$N_{MV,PDO}$ = number of multiple-vehicle PDO crashes per year;
$N_{SV,FI}$ = number of single-vehicle FI crashes per year;
$N_{SV,PDO}$ = number of single-vehicle PDO crashes per year;
$L$ = freeway segment length, mi;
$AADT$ = annual average daily traffic (AADT), veh/day; and
$b_{n,x,y}$ = calibration coefficient for lane count $n$, crash type $x$ (multiple-vehicle or single-vehicle), and crash severity $y$ (FI or PDO).

  Table 1 provides the $b_{n,x,y}$ calibration coefficients for use in Equations 2–5.

**Table 1.  HSM Model Calibration Coefficients.**

| Number of Lanes ($n$) | $b_{n,MV,FI}$ | $b_{n,MV,PDO}$ | $b_{n,SV,FI}$ | $b_{n,SV,PDO}$ |
|---|---|---|---|---|
| 4 | 0.0042 | 0.0014 | 0.1193 | 0.1070 |
| 6 | 0.0037 | 0.0011 | 0.1281 | 0.1029 |
| 8 | 0.0036 | 0.0009 | 0.1374 | 0.0991 |
| 10 | 0.0029 | 0.0007 | 0.1473 | 0.0953 |

Figure 1 shows the HSM SPFs in graphical format. The black lines provide total (FI + PDO) crash frequency, and the red lines provide FI crash frequency. As shown, the models predict that for a given traffic volume, crash frequency will decrease with a larger number of lanes.
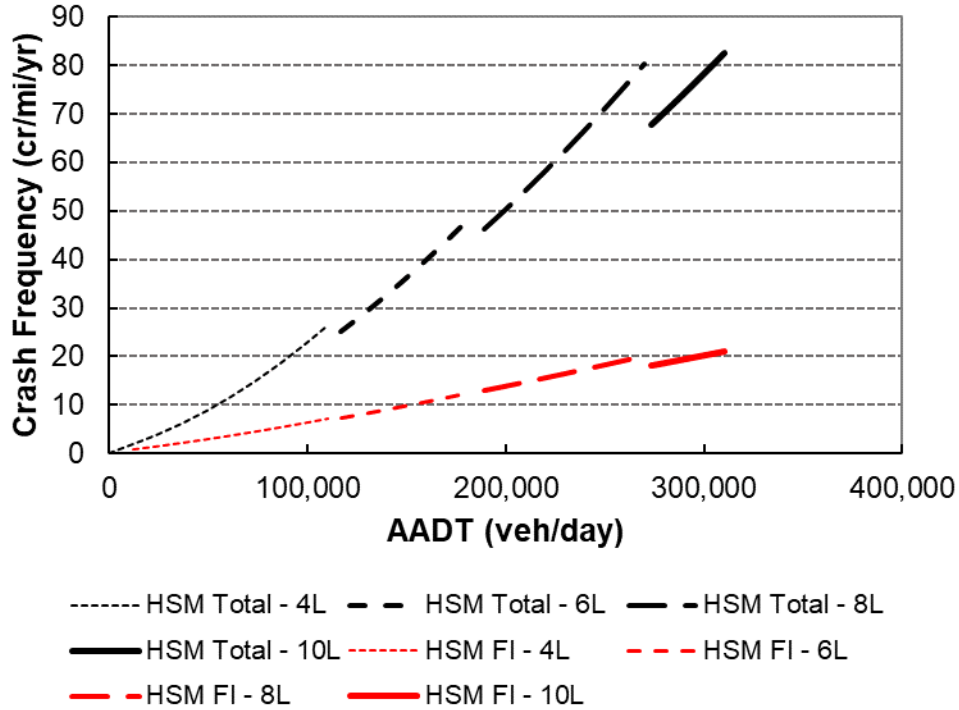


**Figure 1. HSM Models.**

**Texas-Calibrated Models**

TxDOT's *Roadway Safety Design Workbook* contains freeway SPFs that were calibrated using Texas data (*1*). These SPFs provide estimates of base FI crash frequency. Equations 6–8 show the *Workbook* urban freeway SPFs for segments that do not have ramp entrances or exits. The *Workbook* also provides CMFs that allow the analyst to adjust for conditions that differ from the base conditions.

$$N_{FI} = N_{MV,FI} + N_{SV,FI} \tag{6}$$

with:

$$N_{MV,FI} = L \times b_{n,MV,FI} \times \left(\frac{AADT}{1000}\right)^{1.55} \tag{7}$$

$$N_{SV,FI} = L \times b_{n,SV,FI} \times \left(\frac{AADT}{1000}\right)^{0.646} \tag{8}$$

where:
$N_{FI}$ = base number of FI crashes per year.

Table 2 provides the $b_{n,x,y}$ calibration coefficients for use in Equations 7 and 8.

**Table 2. *Workbook* Model Calibration Coefficients.**

| Number of lanes, two-way total ($n$) | $b_{n,MV,FI}$ | $b_{n,SV,FI}$ |
|---|---|---|
| 4 | 0.00532 | 0.13400 |
| 6 | 0.00352 | 0.11900 |
| 8 | 0.00289 | 0.11300 |
| 10 | 0.00220 | 0.10400 |

Figure 2 shows the *Workbook* SPFs in graphical format. As shown, the models predict that for a given traffic volume, crash frequency will decrease with a larger number of lanes.
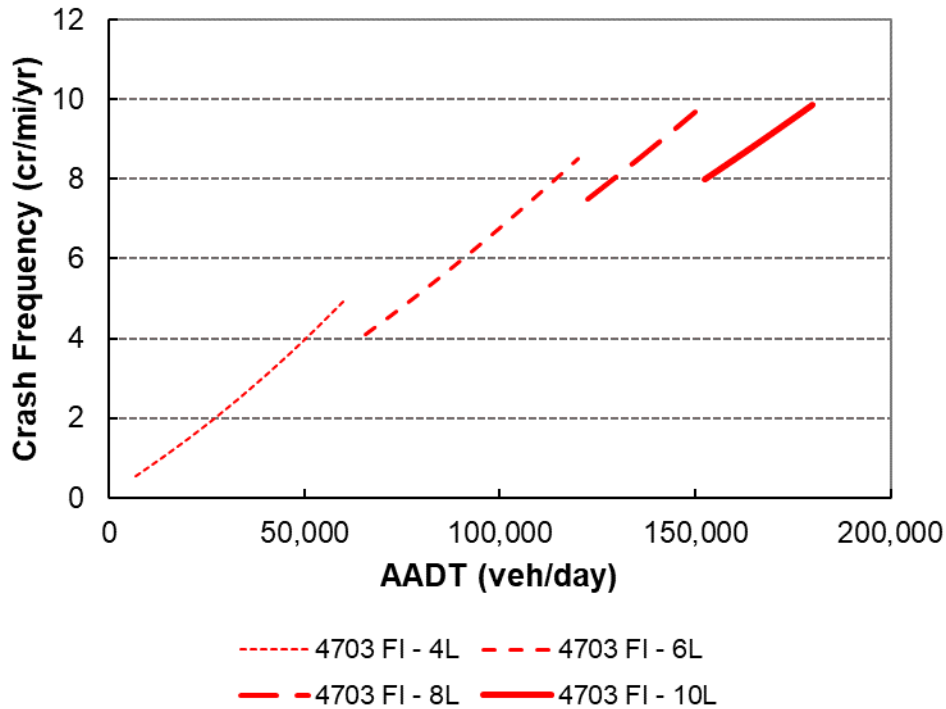


**Figure 2. *Workbook* Models.**

In TxDOT Research Project 0-6811, a new set of SPFs was calibrated for urban freeway segments (*5*). These models are shown in Equations 9 and 10. These models are formulated to provide a one-way crash frequency, considering each roadbed of the freeway separately, such that the distances to upstream and downstream ramps can be independently considered for the two directions of travel. Unlike the preceding models, the 0-6811 SPFs bound to a value of zero (instead of a positive crash frequency) if the distance to the upstream and downstream ramps approaches infinity. These models were calibrated using a dataset of urban freeway segments, and all segments had upstream and downstream ramps within 1.5 miles of the segment.

$$N = 1.0027 \times L \times AADT^{0.539} e^{-1.0243 D_{up} - 1.0877 D_{down} - 0.0241 n_o w_l} \qquad (9)$$

$$N_{KAB} = 0.0514 \times L \times AADT^{0.662} e^{-1.5787 D_{up} - 0.8659 D_{down} - 0.0253 n_o w_l} \qquad (10)$$

where:

| | | |
|---|---|---|
| $N_{KAB}$ | = | number of K, A, and B crashes per year (using the KABCO scale); |
| $D_{up}$ | = | distance to upstream ramp, mi; |
| $D_{down}$ | = | distance to downstream ramp, mi; |
| $n_o$ | = | number of lanes (one-way total); and |
| $w_l$ | = | average lane width, ft. |

Figure 3 shows the 0-6811 SPFs in graphical format. As shown, the models predict that for a given traffic volume, crash frequency will decrease with a larger number of lanes.
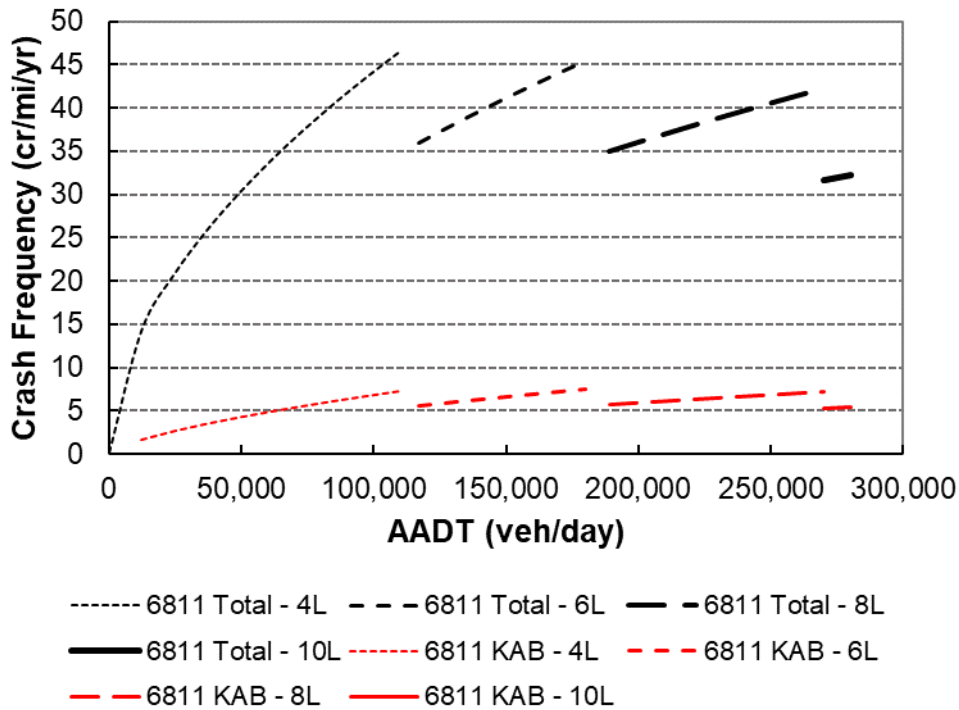


**Figure 3. TxDOT 0-6811 Models.**

More recently, freeway SPFs were calibrated for TxDOT's Beaumont District in TxDOT Implementation Project 5-9052 (*7*). These models are shown in Equations 11 and 12. Figure 4 shows these models graphically. In a manner consistent with the previous models, the Beaumont models show a decrease in crash frequency with a larger number of lanes.

$$N = 6.62 \times 10^{-6} \times L \times AADT^{1.5332} \times e^{-0.0871 n} \qquad (11)$$

$$N_{FI} = 4.30 \times 10^{-6} \times L \times AADT^{1.4731} \times e^{-0.0619 n} \qquad (12)$$
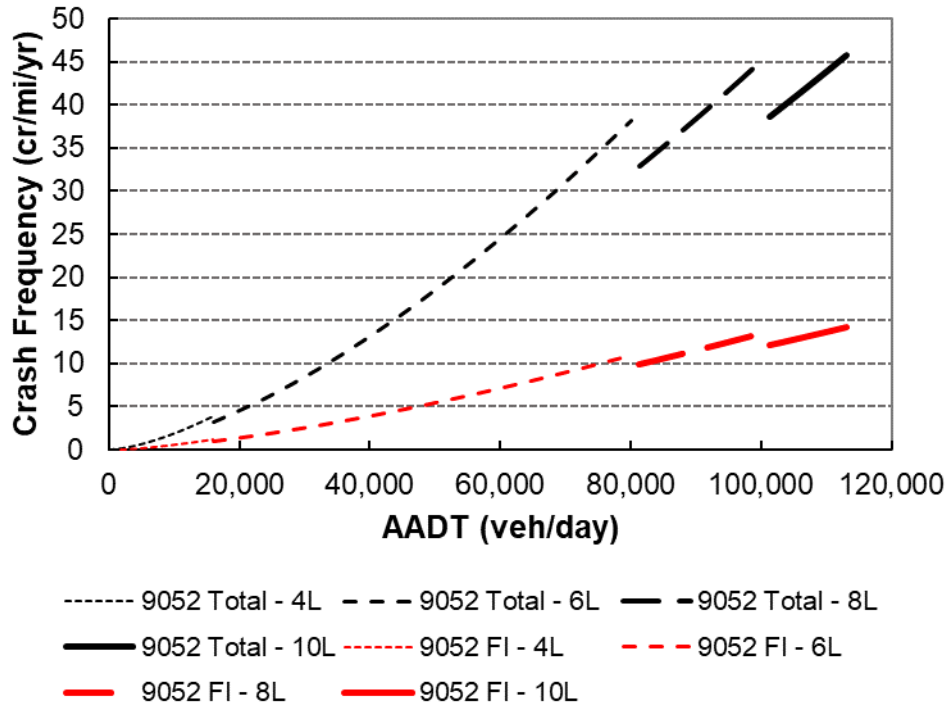
**Figure 4. TxDOT 5-9052 Models.**

**Effect of Cross-Sectional Widths on Safety Performance**

The preceding safety prediction models include lane width as an input variable. A comparison of four lane-width CMFs is shown in Figure 5. Three of the four models showed a similar relationship between lane width and crash frequency. The exception was the models developed in TxDOT Research Project 0-6811, which suggested that lane width had a greater effect on crash frequency. It is important to note that very few variables were included in the SPF, so the lane width may be capturing the effect of other correlated variables.

The preceding safety prediction models also include inside and outside shoulder width as input variables. A comparison of eight shoulder-width CMFs is shown in Figure 6. Note the following observations:

- The findings of TxDOT Research Project 0-4703 suggest that inside shoulders are more influential on crash frequency than outside shoulders. However, the magnitude of the safety effect is relatively minor. The computed CMF values are less than 1.2 (indicating a 20-percent increase in crash frequency) for both outside and inside shoulders even if the width decreases to 1 ft.
- The HSM safety prediction models (i.e., the findings of NCHRP Project 17-45) suggest that outside shoulders are more influential on crash frequency than inside shoulders. The computed CMF values are relatively small for inside shoulders but relatively large for outside shoulders.
- The findings of TxDOT Research Project 0-6811 suggest that outside shoulders are more influential on crash frequency than inside shoulders. The computed CMF values are relatively large for both outside and inside shoulders.

- The findings of TxDOT Implementation Project 5-9052 suggest that the effect of outside shoulder width is similar to that found in TxDOT Research Project 0-4703. This project's findings also suggest that inside shoulder width is notably more influential on crash frequency than what was found in the other research projects.
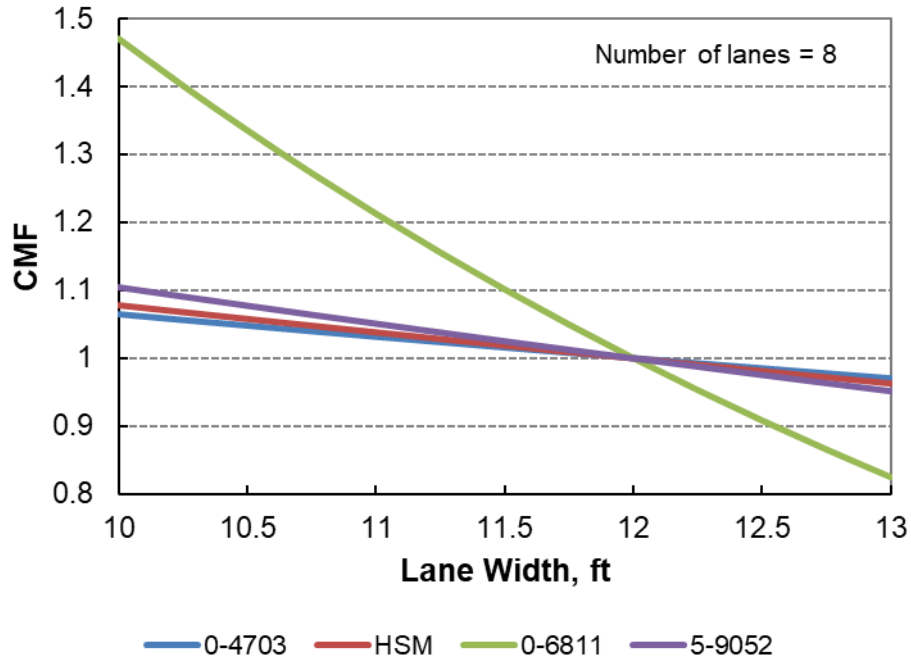


**Figure 5. Lane Width CMFs.**
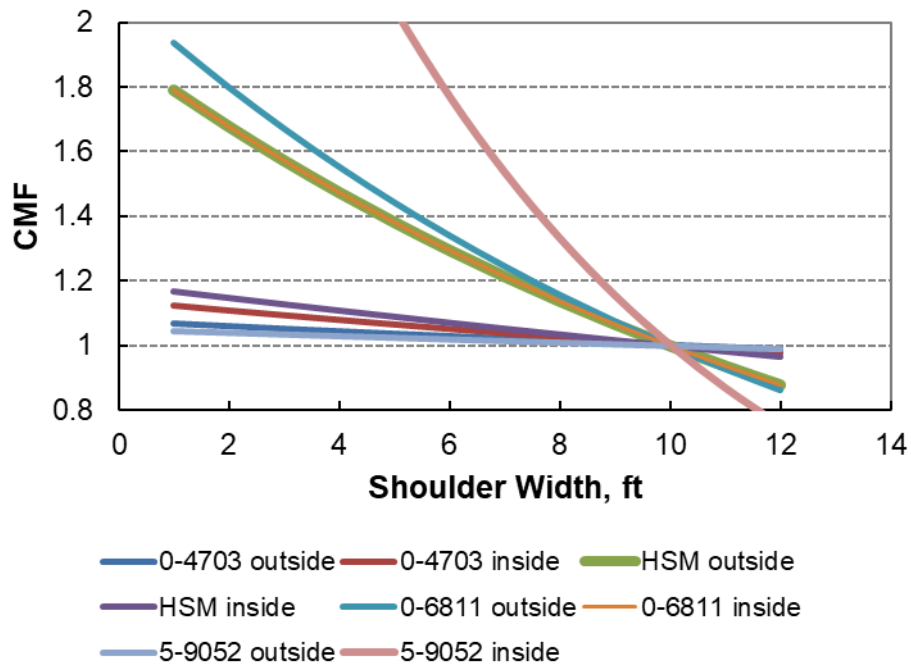


**Figure 6. Shoulder Width CMFs.**

9

In all three research projects, the shoulder width CMFs were developed for all lane counts and as part of a full model calibration effort. That is, the same CMF applied for freeway segments with 4 lanes or 10 lanes.

**Severity Distribution**

The HSM safety prediction models include severity distribution functions (SDFs) to account for the differing effects that some input variables may have on the distribution of crash severity. The following variables are included in the SDF:

- Inside (median) and/or outside (roadside) longitudinal barrier presence.
- Proportion of hours with high traffic volumes (defined as greater than 1000 veh/h/lane).
- Rumble strip presence on the inside and/or outside shoulders.
- Proportion of segment length with horizontal curvature.
- Lane width.
- Area type (rural vs. urban).

Figure 7 shows a graphical representation of the lane width SDF, which illustrates a decrease in the proportion of K crashes and an increase in the proportion of C crashes when lane width increases.
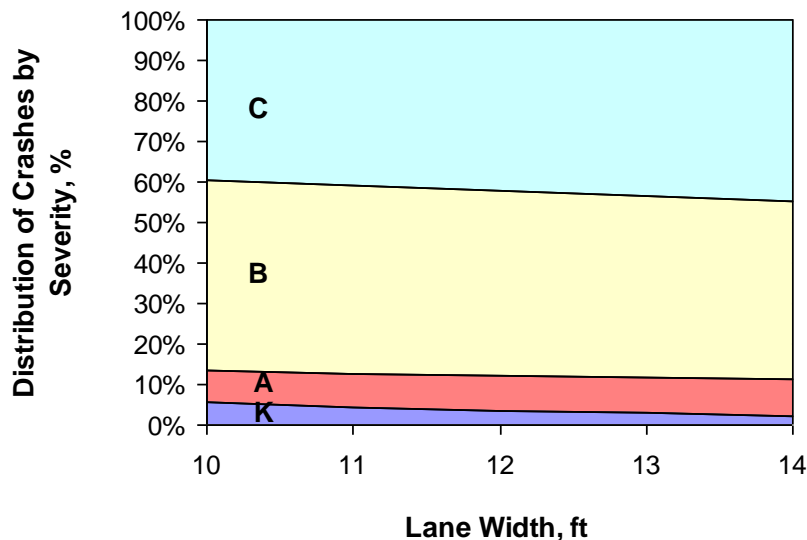


**Figure 7. Lane Width SDF for HSM Models (*3*).**

The safety prediction models from TxDOT Research Project 0-6811 account for severity distribution by providing different CMF coefficient values for the total crash frequency model and the KAB crash frequency model. Similarly, the models from TxDOT Research Project 5-9052 provide different CMF coefficient values for the total crash frequency model and the FI crash frequency model.

## Effects of Lane Count on Safety Performance

Lane count is one of the most important design elements of a roadway. It significantly influences capacity, level of service, operation, and safety. Urban multilane highway facilities are typically designed with 4–8 lanes. With the growth in traffic demand, some urban roadways have been designed or reconstructed with more lanes to increase capacity. While the increase in the number of lanes decreases congestion greatly and less congestion is usually associated with some degree of improved safety, most practicing engineers and transportation planners are concerned that crash rates might increase with the increase in the number of lanes, perhaps due to the tradeoffs that may occur to accommodate the new lanes, such as narrowing lanes or shoulders.

According to the HCM, capacity is proportional to the number of lanes, and as the number of lanes increases, the free-flow speed also increases slightly (*8*). So far, the relationship between number of lanes and safety has not been fully explained by safety researchers, especially when the number of lanes is 11 or more. Some researchers have evaluated the safety effectiveness of lane conversion. Council and Stewart (*9*) compared the safety performance of two- and four-lane roadways. They concluded that the safety effects of converting two-lane roads to four lanes is a crash reduction of 40–60 percent. Some studies, however, have reported opposite results. Milton and Mannering (*10*) developed crash prediction models for principal arterials in Washington State. In the following elasticity analysis, the researchers found that a higher number of lanes is associated with more crashes. To examine whether various changes in road network infrastructure and geometric design can be associated with changes in roadway safety, Noland and Oh (*11*) analyzed the county-level time-series roadway and crash data in Illinois. Increasing the number of lanes was not found to be beneficial for safety. Abdel-Aty and Radwan (*12*) and Kononov et al. (*13*) reported similar findings.

## Managed-Lane Models

Fitzpatrick and Avelar conducted an analysis of managed-lane safety performance, focusing on the cross-sectional elements (*6*). They developed statistical models using a dataset of about 128 miles of freeways with managed lanes in California and about 60 miles of freeways with managed lanes in Texas. Their Texas sites consisted of about 42 miles of freeways with pylon-separated managed lanes and about 18 miles of freeways with managed lanes separated by flush-paved, marked buffers. These sites were located in Dallas (I-635 and US 75) and Houston (US 290, I-10, and US 59). Figure 8 shows a comparison of crash frequencies and buffer width by buffer type. (The crashes include those that occurred on general purpose and managed lanes.) The following two trends are apparent: (a) crash frequency decreases with wider buffers, and (b) crash frequency is higher with pylon-separated managed lanes than with flush-paved managed lanes.
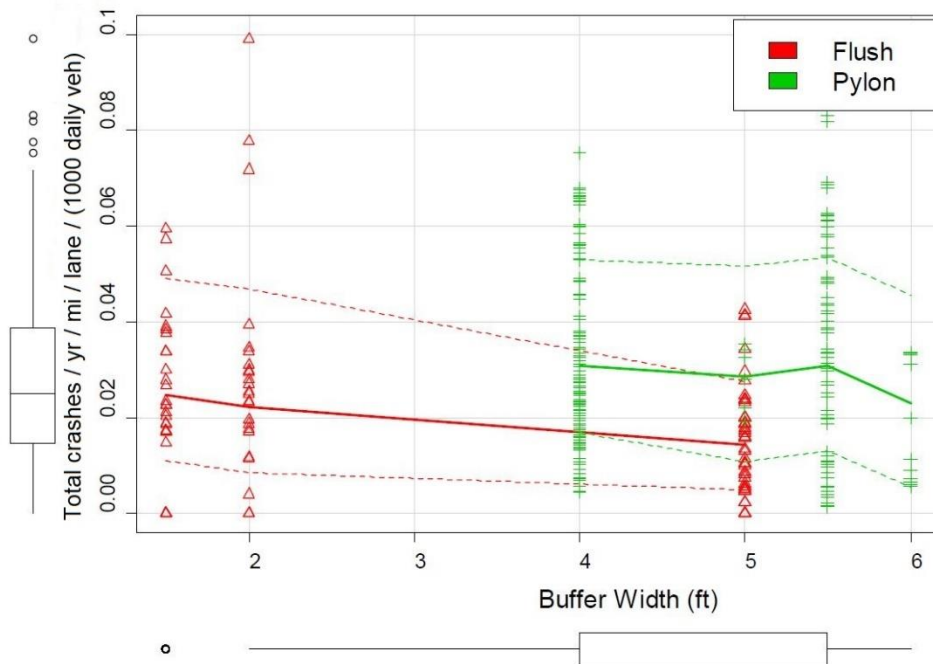
**Figure 8. Safety Effect of Managed-Lane Buffer Type and Width in Texas (*6*).**

Srinivasan et al. analyzed the safety performance of freeways with managed lanes in Florida (*14*). They developed safety prediction models for FI crash frequency and total crash frequency for the following facility types:

- Six-lane freeways with HOV lanes.
- Eight-lane freeways with HOV lanes.
- Ten-lane freeways with HOV lanes.
- Ten-lane freeways with high-occupancy toll (HOT) lanes.
- Twelve-lane freeways with HOV lanes.

Their models account for crashes across the entire cross section, combining the crashes in the general-purpose lanes and the managed lanes.

The authors found that the provision of a marked buffer with more than 2 ft of width would slightly reduce FI crash frequency (see Figure 9a) and the provision of a buffer of any width would slightly reduce total crash frequency compared to providing only a marked stripe (see Figure 9b). These trends are similar to those reported by Fitzpatrick and Avelar (*6*).

a. FI Crash Frequency            b. Total Crash Frequency
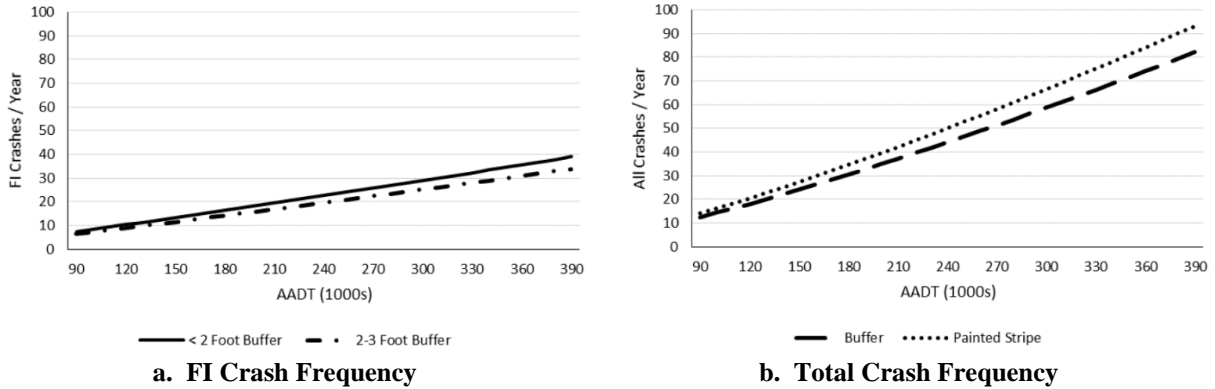
**Figure 9. Safety Effect of Managed-Lane Buffer Type and Width in Florida (*14*).**

## Other Models in the Literature

In addition to the preceding safety prediction models, additional models have been documented to provide more focused analyses of key geometric variables for freeways. Most of these models are applied in a manner similar to those documented in the HSM and similar sources. Additionally, some "real-time" crash prediction models have been developed for the purpose of assisting active traffic safety management systems on freeways.

### Conventional Models

Moon and Hummer (*15*) developed safety prediction models for crashes occurring at influence areas of freeway ramps. The models computed the safety effects of key factors (i.e., traffic, roadway, and environmental) using three statistical models with negative binomial (NB) distribution: (a) a generalized linear model (GLM) with only main effect variables, (b) a GLM with main effects and interaction terms, and (c) a model with the basic functional form recommended by Hauer (*16*) with consideration of various functional forms for each variable.

Re-segmentation is a common practice in the development of crash prediction models. Re-segmentation is the process of defining the roadway facility of interest in terms of homogeneous segments. Instead of re-segmentation, Zheng et al. (*17*) used basic freeway segments in Liaoning, China, with heterogeneous characteristics (geometric and operational) to develop models. Some of the variables include cumulative curvature, cumulative longitudinal gradient, side clearance, and density of traffic signs.

Haq et al. (*18*) developed SPFs for truck crashes along I-80 in Wyoming. Influential variables in the modeling technique included traffic, road geometry characteristics, and weather parameters. Using both continuous count station data and disaggregate INRIX® speed data, Dutta et al. (*19*) assessed the relationship between crashes and quality of flow at different levels of temporal aggregation from rural freeway (four-lane) and urban freeway (six-lane) segments in Virginia. Traffic and speed information at 15-min, hourly, and annual aggregation intervals were used to determine the best-fit measures. Additionally, this study examined the suitability of using speed data to enhance model performance and the data quality between continuous count station and INRIX® data.

13

Das et al. (*20*) used speed and weather data to develop safety performance functions for rural roadways.  They used weather data from the National Oceanic and Atmospheric Administration and 5-minute interval operating speed data from the National Performance Management Research Data Set to develop the models for different rural facility types.  Crash data from the Highway Safety Information System were collected for the states of Washington and Ohio.  For rural interstate models, traffic volume, presence of curve, and average hourly speed showed significance.

*Real-Time Crash Prediction Models*

Real-time crash risk assessment is an emergent analysis topic that can identify risk-prone traffic circumstances and facilitate the implementation of active traffic safety management systems on roadways.  The instantaneous crash probability, measured from these models, can be used to inform road users about road hazard information in real-time as a proactive safety measure.  Hossain and Muromachi (*21*) developed a real-time crash prediction model for urban expressways in Tokyo, Japan, using Bayesian network modeling.  Exploration of surrogate safety measures for traffic collisions in the vicinity of recurring bottlenecks can be used in developing dynamic traffic control methods to prevent crashes.  Chen et al. (*22*) investigated the association between real-time traffic flow rate parameters and the traffic collisions risk at recurring bottleneck areas on freeways in California.  Xu et al. (*23*) evaluated the application of the genetic programming model for real-time crash prediction on freeways in California.  Along with traffic, weather, and crash data, this study utilized the receiver operating characteristic curve to evaluate performance of the models.  Using crash data on a 31-mile-long expressway in China, Ma et al. (*24*) applied both the NB model and random effect negative binomial (RENB) model to estimate crashes.  The maximum likelihood (ML) method was used to determine the parameters, and the mixed stepwise procedure was applied to examine the significance of explanatory variables.  The significant contributing factors were longitudinal grade, width of the roadway, and ratio of longitudinal grade to curve radius.

Roy et al. (*25*) considered one-minute aggregated loop detector data along with detector layouts as input.  They applied a cell transmission model (CTM) to incorporate states of traffic flow variables for a pre-defined hypothetical detector layout.  To improve upon the conventional real-time crash prediction models, this study developed several models using Bayesian networks (BNs) and dynamic Bayesian networks (DBNs) for the network.  Yang et al. (*26*) introduced the Bayesian dynamic logistic regression (LR) to develop the real-time crash model on urban expressways, where the model constraints could dynamically change by effectively incorporating a new occurrence with prior knowledge upon arrival.

In recent years, many researchers developed machine-learning models to improve the precision of crash counts on freeway segments.  Sun et al. (*27*) developed a support vector machine (SVM) with two penalty parameters to estimate real-time crash risk on urban expressway segments in Shanghai, China, by using dual-loop detector data.  Many studies use traffic variables (i.e., speed, volume, density) to predict crash likelihoods, which are not suitable for roads where the traffic conditions are estimated using speed data extracted from sampled floating cars or smart phones.  Sun and Sun (*28*) proposed a DBN model of time sequence traffic data to examine the association between crash occurrence and dynamic speed condition data using data from Shanghai, China.  A close association between traffic states and crashes on

14

expressways is usually anticipated, and the occurrence of crashes may be influenced by the interaction of different groupings of traffic states upstream and downstream from the crash location. Based on the crash data and the corresponding traffic flow detector data collected on expressways in Shanghai, Sun and Sun (*29*) proposed a hybrid model combining an SVM model with a *k*-means clustering algorithm to predict the likelihood of crashes.

Wang and Kim (*30*) considered the probability of crash occurrence as a class variable (output) and applied an artificial neural network (ANN) classifier to predict a crash occurrence within a given area in the network up to three hours into the future. Wang and Feng (*31*) analyzed the real-time crash risk for expressway ramps using roadway, traffic, and demographic data. They developed two Bayesian logistic regression models to identify crash precursors and developed four SVMs that were applied to predict crash occurrence. Both modeling frameworks show that the socio-demographic and trip generation variables outperform their counterparts without those parameters.

## STATISTICAL MODELING METHODS AND ISSUES

Model parameters as used in the HSM and discussed so far are referred to as fixed effects in a broad statistical sense. In general, the coefficients obtained from GLMs can be considered as fixed effects. The variables corresponding to fixed effects are understood to have time-invariant effects or are assumed to affect all sites similarly (e.g., assuming that increasing lane width will reduce crash frequency at all sites), and their effects are estimated and interpreted as metrics of underlying parameters from a latent data-generating process.

In contrast, random effects estimate the influence of factors that are deemed the observed realizations of a random variable. As such, it is typically not of interest to quantify how the response variables shift with the observed realizations in the dataset, but rather to account for the impact of such variations in the model. Consistently with the above definitions, mixed-effects models are those that include both fixed and random effects (*16*). Mixed-effects models can handle repeated measures in cross-sectional data accounting for each unit of data aggregation as random effects (i.e., the blocking units in the data, such as individual study locations with more than one datum in the analysis). This approach allows the inclusion of locations that have experienced changes in their cross section over the period of evaluation. Otherwise, data from such locations would have been partially reduced only in the framework of fixed effects. However, the use of random effects in models adds a longitudinal dimension to the otherwise cross-sectional data structure.

The use of a mixed-effects model has a measurable impact on the point estimate prediction (a right bias) and in the dispersion estimate (underestimation) and thus corrections are needed. After the necessary adjustments, it can be shown (*32*) that the resulting models are compatible with the HSM predictive method framework. Figure 10 demonstrates the improved prediction of a mixed model after adjusting for right bias and underestimated dispersion from a crash prediction application at a large network of highways. The top plot in Figure 10 shows inadequate crash predictive performance of the unadjusted mixed-effects model. Specifically, the dispersion of the predictions is narrower than the dispersion in the observations. In contrast, the middle plot shows the adjusted mixed model with improved dispersion in the prediction.

This performance is very comparable to the simpler NB model shown in the bottom row in Figure 10.
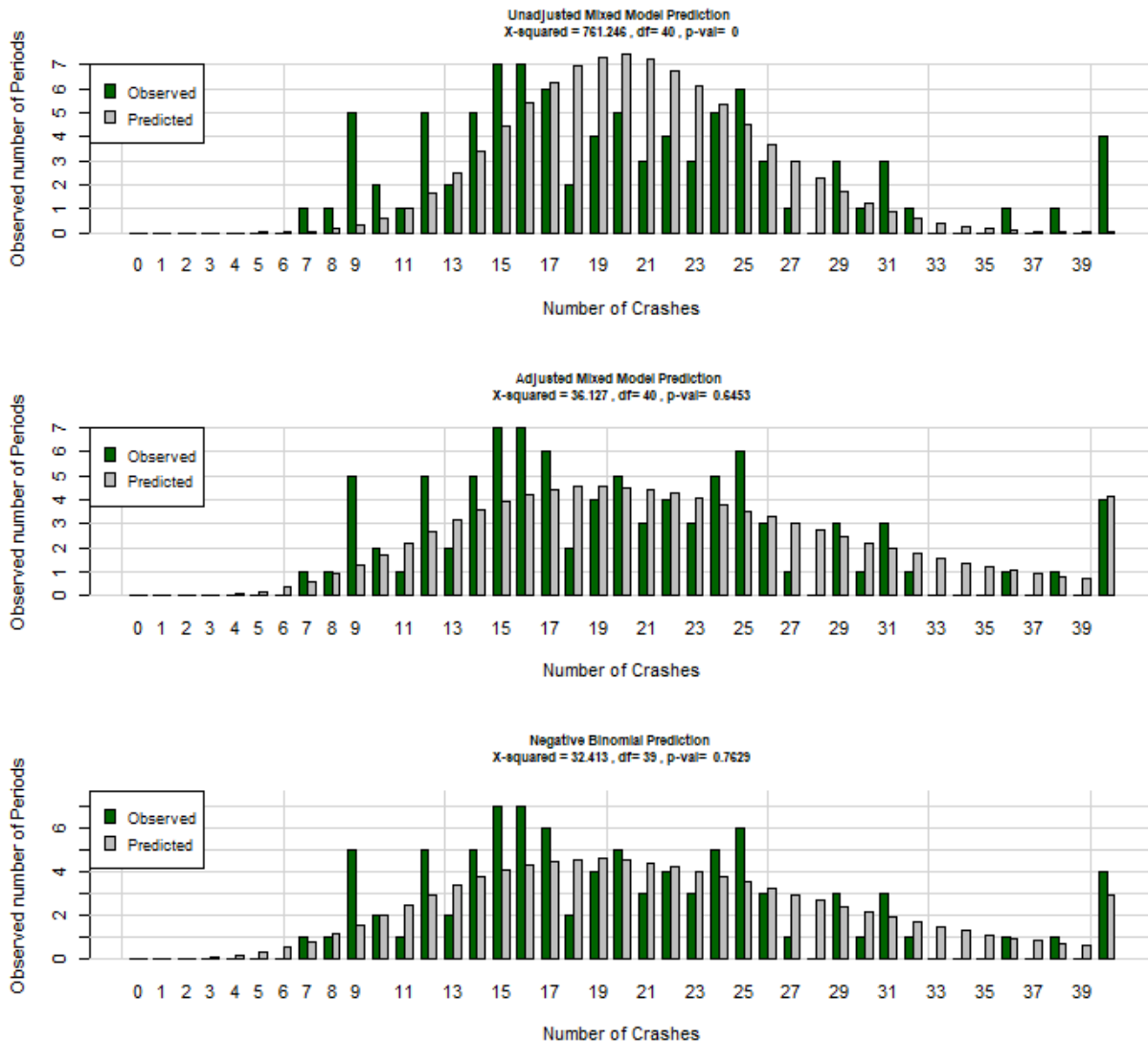


**Figure 10. Predictive Performance of Unadjusted and Adjusted Poisson-Lognormal Mixed-Model Compared to Negative Binomial.**

Safety analyses in the literature have employed a wide variety of modeling approaches. Table 3 provides a list of modeling approaches that differed from the commonly used regression models that yielded the safety prediction models like those in the HSM, the *Workbook*, and TxDOT Research Projects 0-6811 and 5-9052. More detailed discussion of the advantages and disadvantages of the various modeling approaches is available elsewhere (*16*, *33*).

Any model development effort must be evaluated with goodness-of-fit statistics. Several statistics can be used to evaluate model fit. These measures include the following statistics:

- Pearson product-moment correlation coefficient ($R$) and coefficient of determination ($R^2$).
- Mean prediction bias ($MPB$).
- Mean absolute deviation ($MAD$).
- Mean square prediction error ($MSE$).
- Over dispersion parameter-based criterion ($R_a^2$).
- Modified chi-squared statistic ($X_m^2$).

The first four statistics listed are described by Washington and Cheng (*34*) and have been used by many researchers in highway safety. The fifth statistic was developed by Miaou (*35*) and is well-suited to assessing the fit of safety data prediction models based on a NB error structure. The last statistic was used by Pilko et al. (*36*) to evaluate the suitability of merging data from multiple states. Other candidate statistics will be identified during this step.

In addition to the statistics, cumulative residual (CURE) plots can be used to evaluate model fit over the range of each independent variable. These plots are useful for evaluating whether the functional form chosen for the SPF is accurate for all values of the independent variable or whether it over/under predicts for certain ranges (*16*).

**Table 3. Summary of Safety Analysis Modeling Topics.**

| Topic | Source | Data Source and Type | Modeling Approach |
|---|---|---|---|
| Crash Prediction Models | Moon and Hummer (*15*) | Traditional variables (geometry, exposure, etc.) | NB |
| | Zheng et al. (*17*) | New influential variables | NB, ML estimation |
| | Dutta et al. (*19*) | Disaggregate speed data | NB, zero-inflated NB |
| | Das et al. (*20*) | Weather data and disaggregate speed data | NB |
| Real-Time Crash Prediction Models | Hossain et al. (*21*) | Traditional variables | BN |
| | Chen et al. (*22*) | Traditional variables | LR modeling technique |
| | Xu et al. (*23*) | Traditional variables | Genetic programming |
| | Ma et al. (*24*) | Traditional variables | RENB |
| | Roy et al. (*25*) | Traditional variables | BNs, DBNs, CTM |
| | Yang et al. (*26*) | Traditional variables | Bayesian dynamic LR |
| Machine-Learning Models | Sun et al. (*27*) | Traditional variables | SVM |
| | Sun et al. (*28*) | Traditional variables | DBN |
| | Sun et al. (*29*) | Traditional variables | Hybrid SVM |
| | Wang and Kim (*30*) | Traditional variables | ANN |
| | Wang et al. (*31*) | Traditional variables | Bayesian LR and four SVM |

# CHAPTER 3: FREEWAY SAFETY DATABASE PREPARATION

## INTRODUCTION

Safety prediction models currently exist in TxDOT's *Roadway Safety Design Workbook* (*1*) and the HSM (*2*, *3*) for urban freeway segments with 4–10 general-purpose lanes. These lane counts represent a large portion of the urban freeway centerline mileage in Texas. However, the models in the *Roadway Safety Design Workbook* were published in 2009. The models in the HSM were published in 2012 and contain variables for more site conditions, such as high-volume hours and lane changes (affected by volume and distance to nearest ramp entrance and exit), but they were calibrated using data from the states of California, Maine, and Washington. A research effort is needed to calibrate the HSM models to Texas conditions.

Additionally, neither the *Roadway Safety Design Workbook* nor the HSM contain models for urban freeways with 11 or more lanes or freeways with managed lanes (e.g., high-occupancy-vehicle or high-occupancy-toll lanes). These facilities represent a small but growing proportion of the urban freeway mileage in Texas, and planning and design for these facilities is often complex because of the tradeoffs that have to be made between capacity, right-of-way constraints, community impacts, and cost, in addition to safety performance. There is a need to develop models for these facilities so safety performance can be considered in addition to the other factors often considered in the project development process.

This chapter describes efforts undertaken to build a database to develop local calibration factors and new safety prediction models for urban freeway facilities of interest. The chapter is divided into two parts. The first part discusses the database preparation efforts for local calibration factors for urban freeways with 4–10 general-purpose lanes. The second part discusses the database preparation efforts for urban freeways with 12 general-purpose lanes and urban freeways with managed lanes.

## DATABASE PREPARATION FOR LOCAL CALIBRATION FACTORS

Chapter 18 of the HSM contains freeway safety prediction models, and Appendix B of the HSM contains guidance on developing local calibration factors for these models. The guidance calls for new calibration factors to be developed at least every 2–3 years using at least 30–50 sites. The HSM provides separate SPFs for the following crash types:

- Multiple-vehicle (MV) FI crashes.
- MV PDO crashes.
- Single-vehicle (SV) FI crashes.
- SV PDO crashes.

For the FI crash SPFs, the HSM also provides an SDF to distribute predicted FI crashes between the K, A, B, and C categories in the KABCO scale.

The research team queried several TxDOT-maintained databases that are essential to the calibration of local calibration factors. These databases include the Texas Reference Marker (TRM) database, which is the state's roadlog database, and the Crash Record Information

System (CRIS) database, which archives records of crashes on state-maintained roadways. The query of freeway segments in TRM yielded the sample described in Table 4.

**Table 4. Preliminary Distribution of Urban Freeway Mileage in Texas.**

| Segment Category | Number of Lanes | | Number of Segments | Total Length (mi) |
|---|---|---|---|---|
| | General-Purpose | Managed | | |
| General-Purpose Lanes Only | 4 | 0 | 7725 | 2034.6 |
| | 5–6 | 0 | 3889 | 992.6 |
| | 7–8 | 0 | 1205 | 337.9 |
| | 9–10 | 0 | 470 | 101.1 |
| | 11–12 | 0 | 64 | 12.6 |
| | 13–14 | 0 | 25 | 1.9 |
| General-Purpose Lanes and HOV Lanes | Any | 1 | 462 | 97.9 |
| | Any | 2 | 124 | 34.8 |
| General-Purpose Lanes and Toll Lanes | Any | Any | 406 | 137.3 |

The research team used the geolocation data for these freeway segments to plot the segments on aerial photographs and then visually reviewed the segments to verify the segment categories (see the first column of Table 4). An example plotting of six-lane freeway segments in the Dallas/Fort Worth area is shown as the red lines in Figure 11.
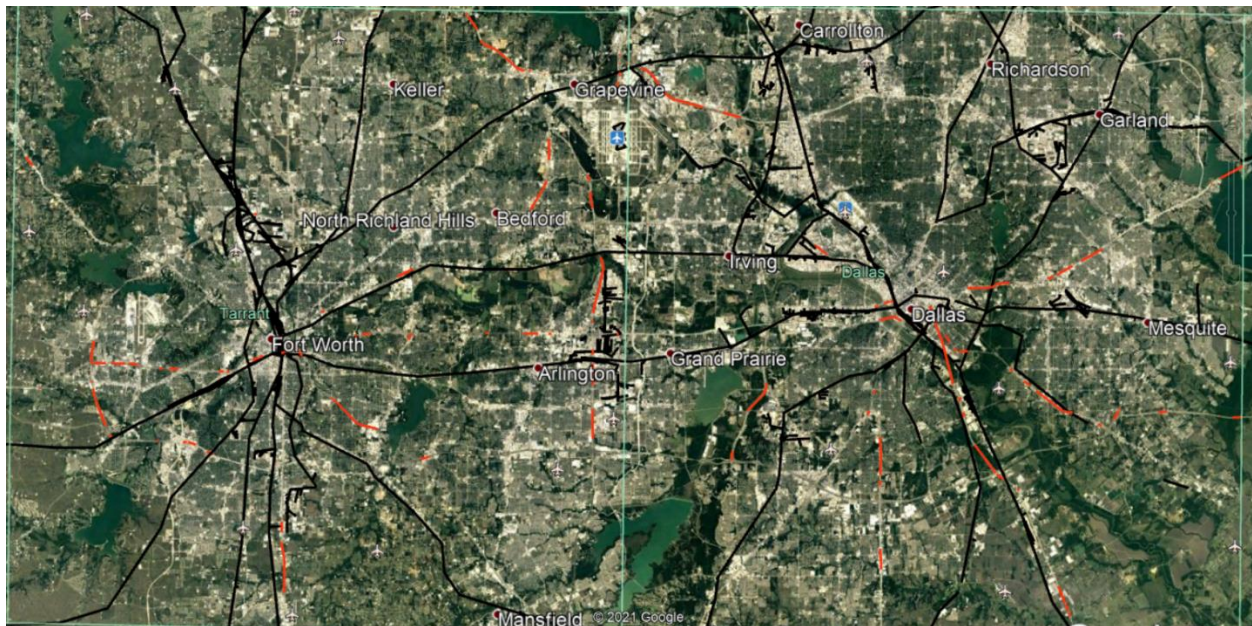


**Figure 11. Example Plotting of Freeway Segments.**

The research team re-categorized the segments by lane count and type. The following lane types were counted: general-purpose, auxiliary, and managed lanes. Auxiliary lanes are identified based on the presence of wide dotted white lane lines as shown in the red box in Figure 12. Managed lanes include HOV, HOT, or toll lanes. Table 5 provides the revised count of urban freeway segments in Texas based on the review of aerial photographs. The totals in Table 5 include segments with no auxiliary or managed lanes and with "typical" geometry. Segments with complex geometry, such as those within system interchanges, are excluded. The

research team obtained the crash counts in Table 5 by merging the TRM data records with CRIS database records for the years 2015–2019.
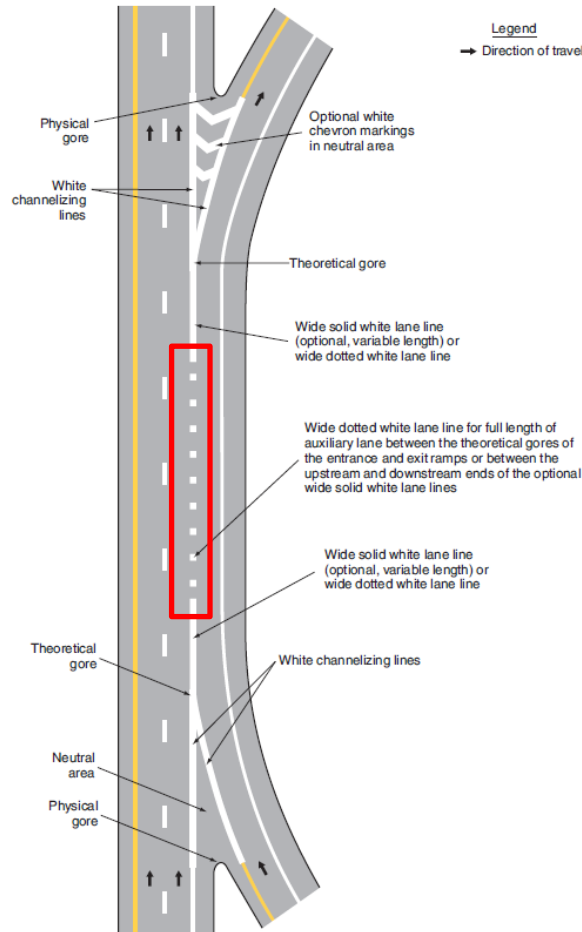


**Figure 12.  Auxiliary Lane Markings (*37*, Figure 3B-10).**

**Table 5.  Revised Count of Urban Freeway Segments without Managed Lanes in Texas.**

| Number of Lanes | Number of Segments | Centerline Miles | Lane-Miles | Crash Count (2015–2019) | | | | |
|---|---|---|---|---|---|---|---|---|
| | | | | Total | MV FI | MV PDO | SV FI | SV PDO |
| 4 | 785 | 280.5 | 1190.7 | 13,285 | 2533 | 5476 | 1667 | 3609 |
| 5–6 | 850 | 292.8 | 1765.9 | 30,693 | 7169 | 15,083 | 3018 | 5423 |
| 7–8 | 553 | 154.9 | 1195.9 | 34,521 | 9198 | 18,151 | 2688 | 4484 |
| 9–10 | 188 | 36.5 | 325.1 | 14,317 | 3619 | 8487 | 762 | 1449 |
| 11–12 | 24 | 3.8 | 33.4 | 1521 | 405 | 854 | 86 | 176 |

The distributions in Table 5 show that freeway segments with 4–6 lanes are the most abundant in terms of centerline mileage and lane-mileage.  As expected, wider segments are less common, but the wider segments have a larger number of crashes due to the higher traffic volumes on these segments.

For all segments in the dataset, the research team was able to obtain the key exposure variables (i.e., traffic volume and segment length) and the five-year crash count.  These variables alone are sufficient to compute local calibration factors for SPFs.  The research team further

identified a subset sample of 50 segments each with 4, 6, 8, and 10 general-purpose lanes for the purpose of conducting more detailed examinations including the geometric and traffic control variables that are used to apply the CMFs that accompany the SPFs.  Table 6 lists the SPFs, their corresponding CMFs, and the primary sources for obtaining the data needed to apply the CMF.

**Table 6.  Freeway SPFs and Corresponding CMFs.**

| SPF | CMF Description | Primary Data Source |
|---|---|---|
| MV or SV crashes | Horizontal curve | Aerial photographs |
| | Lane width | TRM database |
| | Inside shoulder width | TRM database |
| | Median width | TRM database |
| | Median barrier | Aerial photographs, street-level photographs |
| | High volume | Traffic Management Center data |
| MV crashes | Lane change | Aerial photographs |
| SV crashes | Outside shoulder width | TRM database |
| | Shoulder rumble strip | Street-level photographs |
| | Outside clearance | Aerial photographs |
| | Outside barrier | Aerial photographs, street-level photographs |
| Ramp-related crashes | Ramp entrance/exit | Aerial photographs |

The research team plotted the subset sample segments and reviewed aerial photographs to obtain and plot the locations of features relevant to some of the CMFs.  These features included longitudinal barriers (median or outside) and the presence of ramp entrances or exits.  Figure 13 shows plotted placemarks that identify the locations of several barrier pieces on a six-lane freeway segment.



**Figure 13.  Longitudinal Barrier Presence.**

## DATABASE PREPARATION FOR NEW SAFETY PREDICTION MODELS

The HSM contains safety prediction models for urban freeway segments with up to 10 general-purpose lanes and no managed lanes.  Since there are a growing number of segments

with more than 10 general purpose lanes or segments with managed lanes, the research team assembled datasets to describe these segments for the purpose of developing new safety prediction models. The following subsections describe the research team's efforts to develop these datasets.

**Wide Segments without Managed Lanes**

The research team identified a small sample of segments with more than 10 general-purpose lanes. These segments are listed in the bottom row of Table 5. As shown, the number of these segments is small—16 segments, totaling 2.2 centerline miles. However, even with a small sample, a notable number of crashes (1086) was observed on these segments in the queried years (2015–2019) because of the high volumes on these segments. Because the number of wide segments is small, the research team included all these identified segments in the subset sample for detailed analysis (i.e., to extract all geometric and traffic control variables from aerial and street-level photography sources).

**Segments with Managed Lanes**

*Site Identification*

The research team queried the TRM database and reviewed data sources from a previous analysis conducted by TTI for TxDOT's Dallas District to identify 35 continuous sections of urban freeway with managed lanes. These sections are listed in Table 7. Most of the sections are located in the Dallas/Fort Worth or Houston areas, with one (SL 1) located in the Austin area. The research team included all sections in the subsequent data assembly efforts except the SL 1 section in Austin and four others for which traffic volume data were unavailable. In total, the research team included 29 sections totaling about 222 centerline miles.

Previous efforts to analyze the safety of managed-lane facilities focused on the overall facility, analyzing the general-purpose lanes and managed lanes as a single facility (*6*). The research team examined the crash and traffic volume data sources to determine if it would be possible to develop separate safety prediction models for the general-purpose lanes and managed lanes. This type of analysis would require separate traffic volumes for the two lane groups and a method to assign crashes to the two lane groups.

*Traffic Volume Data*

The research team obtained archived traffic counts for the Houston-area managed-lane facilities (*38*). These counts included quarterly inbound and outbound volumes for the various facilities at several key locations along the facility length, hourly volumes for December 2019, and the distribution of volumes by vehicle type (i.e., carpool, vanpool, bus, or motorcycle) for December 2019. The research team obtained similar data for the Dallas-area managed-lane facilities for the years 2017, 2018, or 2019 from TxDOT's Toll Operations Division or the operators of the managed-lane facilities.

**Table 7. Freeway Sections with Managed Lanes.**

| | | Cross Streets | | Length | Buffer | Managed |
|---|---|---|---|---|---|---|
| | **Highway** | **From** | **To** | **(mi)** | **Type** | **Lane Type** |
| Dallas/Fort Worth | US 75 | W Bethany Dr | Ruisseau Dr | 3.5 | Pylons | HOV |
| | US 75 | Galatyn | Midpark | 4.2 | Pylons | HOV |
| | US 75 | Midpark | I-635 | 1 | Barrier | HOV |
| | I-635 | Oates Dr/I-30 | Greenville Ave | 9 | Pylons | HOT |
| | I-635 | Greenville Ave | Luna Rd | 9 | Barrier | HOT |
| | I-35E | Turbeville Rd | PGB Turnpike | 12 | Barrier | HOT |
| | I-35E | PGB Turnpike | I-635 | 5.5 | Barrier | HOT |
| | I-35E | I-635 | LP 12 | 3.5 | Barrier | HOT |
| | I-35W | N Tarrant Pkwy | SH 183 | 7.5 | Barrier | HOT |
| | I-35W | SH 183 | US 280 | 2.5 | Barrier | HOT |
| | SH 114 | SH 26 | Main St | 1.1 | Barrier | HOT |
| | SH 114 | Main St | Texan Trail | 1 | Barrier | HOT |
| | SH 114 | Texan Trail | International Pkwy | 1 | Barrier | HOT |
| | SH 114 | International Pkwy | PGB Turnpike | 4.5 | Barrier | HOT |
| | SH 114 | PGB Turnpike | NW Highway | 1.5 | Barrier | HOT |
| | SH 114 | NW Highway | Rochelle Blvd | 2 | Barrier | HOT |
| | I-820 | SH 183 | I-35W | 6 | Barrier | HOT |
| | SH 183 | I-820 | Industrial Blvd | 6 | Barrier | HOT |
| | SH 183 | Industrial Blvd | McArthur Blvd | 8 | Barrier | HOT |
| | SH 183 | McArthur Blvd | Regal Row | 5 | Barrier | HOT |
| | SL 12 | NW Hwy | SH 183 | 2 | Barrier | HOT |
| | I-30 | Duncan Perry Rd | Postal Way | 10 | Barrier | HOT |
| | I-30 | Postal Way | Hardwick St | 2.4 | Barrier | HOT |
| | I-30 | I-45 | NW Highway | 10 | Barrier (movable) | HOV |
| Houston | I-10 | Westgreen Blvd | SH 6 | 5.5 | Pylons | HOV |
| | I-10 | SH 6 | 1-610 | 12 | Pylons | HOT |
| | I-45 | River Plantation | Parramatta Ln | 15.5 | Stripe | HOV |
| | I-45 | Parramatta Ln | I-10 | 18.5 | Barrier | HOT |
| | I-45 | Emancipation Ave | Rogers Dr | 20 | Barrier | HOT |
| | I-45 | Medical Center Blvd | S Texas Ave | 1 | Stripe | HOV |
| | I-69 | Riverbrook Dr | W Airport Blvd | 13 | Stripe | HOV |
| | I-69 | W Airport Blvd | Alabama St | 14 | Barrier | HOT |
| | I-69 | Hamblen Rd | I-10 | 20 | Barrier | HOT |
| | US 290 | Mason Rd | I-610 | 22 | Barrier | HOT |
| Austin | SL 1 | Lake Austin Blvd | Parmer Ln | 11 | Pylons | HOT |

*Crash Data*

The research team analyzed the CRIS records and determined that additional information would be needed to assign the crashes to general-purpose lanes or managed lanes. The research team obtained the crash reports for the crashes on these facilities, including the narratives, so they could determine which crashes involved managed lanes. The research team obtained more

than 22,000 crash reports for the Dallas-area facilities and more than 33,000 crash reports for the Houston-area facilities.

The research team analyzed the CRIS records using an automated algorithm that searches the narratives for keywords that identify the crash as being related to the managed lanes. Figure 14 shows a screenshot of the user interface for the algorithm. The algorithm uses optical character recognition technology to digitize the crash narratives, searches the narratives for keywords of interest that are specified by the user, and flags narratives that contain one or more of the keywords. The algorithm is not case-sensitive and is able to find keywords within larger words (e.g., the abbreviation HOV could be identified within the word "shove").
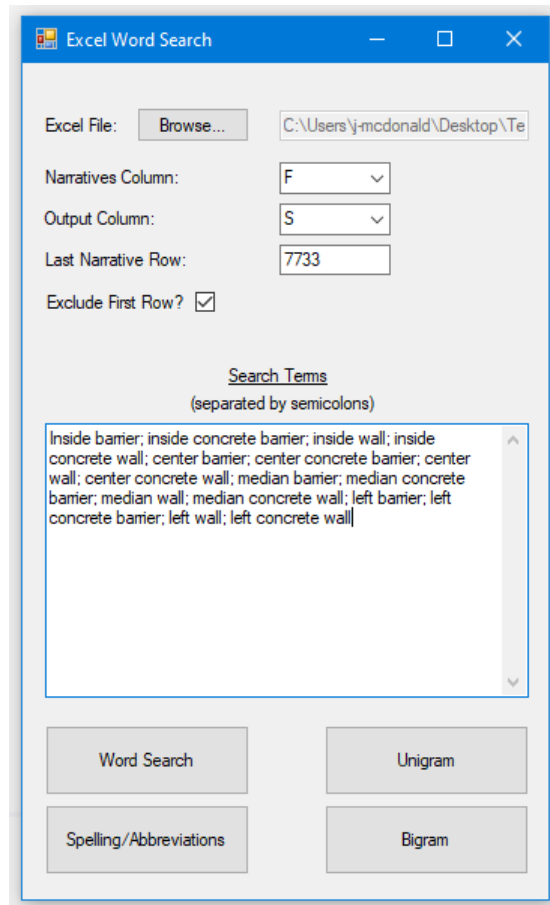


**Figure 14.  Crash Report Analysis Algorithm Interface.**

The research team identified a list of keywords for the managed-lane facilities and ran the algorithm to flag crashes that were managed lane–related. Some of these keywords apply to managed lanes in general (e.g., HOV or HOT), others are specific to the facilities (e.g., TEXpress for Dallas-area facilities), and others are bigrams or multiple-word phrases. The bigrams in the query are shown in Figure 14. The count of identified keywords is provided in Table 8. For US 75, the query included three years of crash data; for the rest of the facilities, the query included one year of crash data. There were a small number of cases where the algorithm could not read the crash narrative, such as if the police officer handwrote the narrative, it was an older-style crash narrative, there was a blank page at the beginning of the narrative, or the crash

narrative was on a separate attached page.  The research team manually checked the crash narratives in all these cases.

**Table 8.  Managed Lane–Related Crash Keyword Counts.**

| | | Crash Narrative Keyword Occurrences by Facility | | | | | |
| | | I-30 | | I-35E | I-635 | | US 75 |
| | Keywords | Duncan Perry—Postal Way | Postal Way—Beckley | President George Bush Turnpike (PGBT)—I-635 | Greenville—Oates | E Luna Rd—Greenville | I-635—Gatalyn, Park Blvd—Bethany |
|---|---|---|---|---|---|---|---|
| 1 | HOV, H.O.V. | 2 | 0 | 11 | 239 | 26 | 589 |
| 2 | HOT, H.O.T. | 0 | 0 | 0 | 0 | 0 | 0 |
| 3 | Toll | 4 | 0 | 4 | 1 | 22 | 0 |
| 4 | Managed lane | 0 | 0 | 0 | 1 | 0 | 0 |
| 5 | ML | 0 | 0 | 0 | 0 | 0 | 0 |
| 6 | Express, expres | 11 | 0 | 33 | 13 | 83 | 12 |
| 7 | Express lane | 8 | 0 | 30 | 8 | 7 | 1 |
| 8 | Texpress, txpress, txpres, tx press, tx pres | 3 | 0 | 2 | 3 | 54 | 1 |
| 9 | Diamond | 0 | 0 | 0 | 0 | 0 | 0 |
| 10 | Carpool, car pool | 0 | 0 | 0 | 0 | 0 | 0 |
| 11 | Pylon | 0 | 0 | 0 | 16 | 0 | 159 |
| 12 | Bigram | 29 | 7 | 17 | 32 | 38 | 63 |
| | Total: | 57 | 7 | 97 | 314 | 230 | 825 |

The research team compared the results in Table 8 with the results of an earlier analysis conducted for TxDOT's Dallas District in a different project (*39*).  The previous analysis was conducted by merging CRIS records with archived incident data from the Traffic Management Center to pre-filter crashes that may be managed lane–related and then reviewing the pre-filtered crash narratives manually to verify that they occurred in the managed lanes or the adjacent general-purpose lane.  Table 9 provides a comparison of the crash counts obtained from the algorithm-based method and the previously used manual methods.  Note that the totals for keywords 1–12 in Table 9 are smaller than the totals in the bottom row of Table 8 because a crash would be counted more than once in Table 8 if its narrative contains more than one of the keywords.

The last two rows of Table 9 show the differences between the processes when only using keywords 1–11 or all keywords 1–12.  The comparisons are reasonable for the I-30 and I-35E facilities.  Somewhat larger differences are apparent for the I-635 facilities and the US 75 facility.  Examination of the differences revealed that there were some errors in the manual method with the assignment of crashes between the two I-635 facilities and potentially many overlooked crashes at the US 75 facility.

**Table 9. Comparison of Algorithm and Manual Crash Identification Methods.**

| Crash Count | Managed Lane–Related Crash Count by Facility | | | | | |
| --- | --- | --- | --- | --- | --- | --- |
| | I-30 | | I-35E | I-635 | | US 75 |
| | Duncan Perry—Postal Way | Postal Way—Beckley | PGBT—I-635 | Greenville—Oates | E Luna Rd—Greenville | I-635—Gatalyn, Park Blvd—Bethany |
| Keywords 1–11 | 16 | 0 | 35 | 249 | 128 | 599 |
| Keyword 12 | 29 | 7 | 14 | 19 | 30 | 33 |
| Keywords 1–12 | 45 | 7 | 49 | 268 | 158 | 632 |
| Manual method | 19 | 2 | 33 | 303 | 91 | 151 |
| Difference (keywords 1–11—manual) | −3 | −2 | 2 | −54 | 37 | 448 |
| Difference (keywords 1–12—manual) | 26 | 5 | 16 | −35 | 67 | 481 |

The research team concluded that the keyword-based algorithm process produces reliable results. However, it should be used carefully and with the following considerations:

- Keywords should be adjusted to include local street and facility names such as TEXpress, TX press, etc., as needed.
- Spot checks/investigations should be done when there is a high concentration of occurrences (i.e., higher crashes/mile) or possibly when there is little to no crashes over a longer distance/period of time when they are expected.

The research team applied this process to managed-lane corridors in the Dallas and Houston areas. The corridors are listed in Table 10. The results of the crash assignment process are shown in Table 11.

**Table 10. Managed-Lane Corridor Locations.**

| Corridor Number | Highway Number | Corridor Start | Corridor End | Crash Data Range |
|---|---|---|---|---|
| 1 | US 75 | W Bethany Dr. | Ruisseau Dr | 2015–2019 |
| 2 | US 75 | Galatyn | Midpark | 2015–2019 |
| 3 | US 75 | Midpark | I-635 | 2015–2019 |
| 4 | I-635 | Oates Dr/I-30 | Greenville Ave | 2015–2019 |
| 5 | I-635 | Greenville Ave | Luna Rd | 2015–2019 |
| 6 | I-35E | Turbeville Rd | PGBT | 5/20/2017–2019 |
| 7 | I-35E | PGBT | I-635 | 2015–2019 |
| 8 | I-35E | I-635 | LP 12 | 12/8/2015–2019 |
| 9 | I-35W | N Tarrant Pkwy | SH 183 | 7/20/2017–2019 |
| 10 | I-35W | SH 183 | US 280 | 4/5/2018–2019 |
| 13 | SH 114 | Texan Trail | International Pkwy | 2015–2019 |
| 14 | SH 114 | International Pkwy | PGBT | 11/4/2017–2019 |
| 15 | SH 114 | PGBT | NW Hwy | 11/4/2017–2019 |
| 16 | SH 114 | NW Hwy | Rochelle Blvd | 11/4/2017–2019 |
| 17 | I-820 | SH183 | I-35W | 2015–2019 |
| 18 | SH-183 | I-820 | Industrial Blvd | 10/27/2018–2019 |
| 19 | SH-183 | Industrial Blvd | McArthur Blvd | 10/27/2018–2019 |
| 20 | SH-183 | McArthur Blvd | Regal Row | 10/27/2018–2019 |
| 21 | SL 12 | NW Hwy | SH 183 | 10/27/2018–2019 |
| 22 | I-30 | Duncan Perry Rd | Postal Way | 2015–2019 |
| 23 | I-30 | Postal Way | Hardwick St | 2015–2019 |
| 25 | I-10 | Westgreen Blvd | SH-6 | 2015–2019 |
| 26 | I-10 | SH 6 | I-610 | 2015–2019 |
| 27 | I-45 | River Plantation | Parramatta Ln | 11/1/2016–2019 |
| 28 | I-45 | Parramatta Ln | I-10 | 2015–2019 |
| 29 | I-45 | Emancipation Ave | Rogers Dr | 2015–2019 |
| 31 | I-69 | Riverbrook Dr | W Airport Blvd | 2015–2019 |
| 32 | I-69 | W Airport Blvd | Alabama St | 2015–2019 |
| 33 | I-69 | Hamblen Rd | I-10 | 2015–2019 |

**Table 11. Managed-Lane Crash Allocation Analysis Results.**

| Corridor Number | Crash Totals | | | |
| --- | --- | --- | --- | --- |
| | Preliminary (all lanes) | Flagged for Manual Check | Identified as False Positive (not in managed lanes) | True Managed-Lane Crashes |
| 1 | 931 | 51 | 37 | 207 |
| 2 | 1852 | 5 | 22 | 772 |
| 3 | 305 | 17 | 19 | 28 |
| 4 | 3921 | 366 | 55 | 1280 |
| 5 | 4836 | 8 | 128 | 551 |
| 6 | 693 | 2 | 31 | 46 |
| 7 | 2011 | 149 | 49 | 83 |
| 8 | 1886 | 1008 | 155 | 32 |
| 9 | 693 | 2 | 28 | 52 |
| 10 | 574 | 0 | 18 | 29 |
| 13 | 319 | 1 | 10 | 8 |
| 14 | 122 | 1 | 3 | 12 |
| 15 | 64 | 0 | 6 | 22 |
| 16 | 61 | 0 | 0 | 1 |
| 17 | 964 | 29 | 23 | 67 |
| 18 | 97 | 0 | 14 | 20 |
| 19 | 384 | 6 | 20 | 45 |
| 20 | 154 | 2 | 10 | 17 |
| 21 | 69 | 4 | 4 | 5 |
| 22 | 1855 | 312 | 22 | 53 |
| 23 | 663 | 393 | 34 | 4 |
| 25 | 1361 | 2 | 7 | 182 |
| 26 | 5162 | 138 | 79 | 361 |
| 27 | 2852 | 35 | 213 | 196 |
| 28 | 9750 | 40 | 40 | 185 |
| 29 | 7958 | 31 | 114 | 106 |
| 31 | 290 | 99 | 11 | 42 |
| 32 | 4439 | 10 | 110 | 100 |
| 33 | 1878 | 65 | 39 | 58 |
| Total | 56,144 | 2776 | 1301 | 4564 |

The research team assigned the managed-lane crashes to the TRM-defined segments for modeling. Table 12 shows the distribution of crashes across the analysis segments by type and severity.

*Geometric Data*

The research team obtained geometric variables for the managed-lane segments from the TRM database and aerial photography sources. Table 13 shows the distribution of values for key geometric variables. The research team collected additional variables but found that they lacked sufficient variation to be useful in modeling efforts.

**Table 12. Managed-Lane Crash Distribution.**

| Facility Type | Number of Segments | Crash Type and Severity | Crash Count Statistic | | |
|---|---|---|---|---|---|
| | | | Mean | Standard Deviation | Range |
| Non-reversible | 262 | SV-FI | 0.72 | 1.97 | 0–18 |
| | | SV-PDO | 1.08 | 2.94 | 0–33 |
| | | MV-FI | 0.89 | 1.96 | 0–19 |
| | | MV-PDO | 1.38 | 3.12 | 0–24 |
| Reversible | 230 | SV-FI | 0.35 | 0.80 | 0–5 |
| | | SV-PDO | 0.49 | 0.97 | 0–6 |
| | | MV-FI | 0.58 | 1.76 | 0–15 |
| | | MV-PDO | 0.80 | 1.86 | 0–13 |

**Table 13. Managed-Lane Geometric Variable Distribution.**

| Facility Type | Geometric Variable | Variable Statistic | | |
|---|---|---|---|---|
| | | Mean | Standard Deviation | Range |
| Non-reversible | Inside shoulder width (ft) | 6.2 | 5.2 | 0.0–23.5 |
| | Outside shoulder width (ft) | 4.6 | 4.7 | 0.0–20.0 |
| | Access weaving section density (sections/mi) | 0.1 | 0.5 | 0.0–3.9 |
| | Access ramp density (gores/mi) | 0.6 | 2.0 | 0.0–13.2 |
| Reversible | Average shoulder width (ft) | 2.5 | 1.3 | 0.0–7.0 |
| | Access ramp density (gores/mi) | 0.5 | 1.7 | 0.0–16.1 |

Figure 15 shows two types of access weaving sections on an example freeway segment. The managed lanes are accessed via weaving sections in both directions of travel, with the weaving occurring in the general-purpose lanes on the top portion of the drawing and in the managed lanes on the bottom portion of the drawing. Both weaving sections are counted toward the total, and they would be counted even if they extended past the segment endpoints. The four circled gores are counted toward the total number of access ramp gores. Access ramp gores in the managed lanes are not counted if they connect to an access weaving section in the managed lanes, as shown in the bottom portion of the drawing.
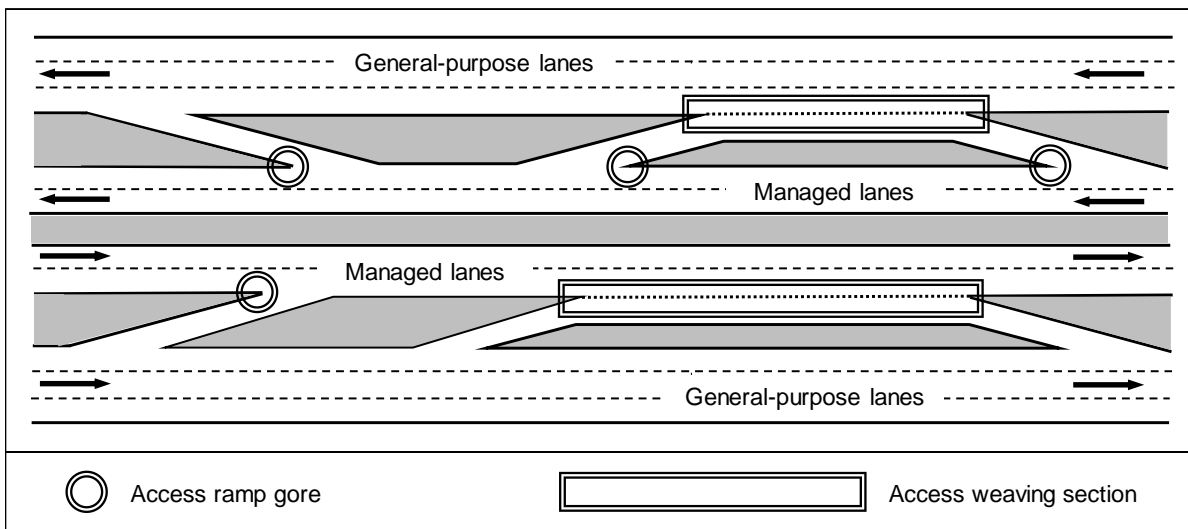


**Figure 15. Example Access Weaving Sections.**

# CHAPTER 4: FREEWAY SAFETY DATA ANALYSIS

## INTRODUCTION

Safety prediction models in sources like TxDOT's *Roadway Safety Design Workbook* (*1*) and the HSM (*2, 3*) can be used to predict crash frequency for urban freeway segments with 4–10 general-purpose lanes. These lane counts represent a large portion of the urban freeway centerline mileage in Texas. Neither of these sources contains models for urban freeways with 11 or more lanes or freeways with managed lanes (e.g., high-occupancy-vehicle or high-occupancy-toll lanes). These facilities represent a small but growing proportion of the urban freeway mileage in Texas. There is a need to develop models for these facilities so safety performance can be considered in addition to the other factors often considered in the project development process.

This chapter describes efforts to analyze a database developed to compute local calibration factors and new safety prediction models for urban freeway facilities of interest. This chapter is divided into three parts. The first part discusses efforts to compute local calibration factors to apply the HSM models to urban freeways with 4–10 general-purpose lanes and to extend these models to urban freeways with up to 12 general-purpose lanes. The second part discusses efforts to calibrate new safety prediction models for managed-lane facilities on urban freeways. The third part provides guidance for applying the local calibration factors and new models.

## COMPUTATION OF LOCAL CALIBRATION FACTORS

Chapter 18 of the HSM contains freeway safety prediction models for the following crash types:

- MV FI crashes.
- MV PDO crashes.
- SV FI crashes.
- SV PDO crashes.

For the FI crash SPFs, the HSM also provides an SDF to distribute predicted FI crashes between the K, A, B, and C categories in the KABCO scale.

### Calculation Method

Appendix B of the HSM contains guidance on developing local calibration factors for these models. The guidance calls for new calibration factors to be developed at least every 2–3 years using at least 30–50 sites. This procedure involves assembling a set of segments, obtaining the observed crash count on the segments for a given time period, computing the predicted crash count for the same time period using the HSM models, and computing the ratio of observed to predicted crashes. A separate ratio *C* is computed for each SPF using the following equation:

$$C = \frac{\sum_{i=1}^{n} y_i}{\sum_{i=1}^{n} \hat{y}_i} \tag{13}$$

where:

$y_i$ = observed annual crash frequency for site $i$;
$\hat{y}_i$ = predicted annual crash frequency for site $i$; and
$n$ = number of sites.

The predicted crashes are then adjusted to calculate the calibrated predicted crash frequency $\mu_i$:

$$\mu_i = C\hat{y}_i \tag{14}$$

Others, including Alluri et al. (*40*), have suggested a larger sample for calibration factor development.

For this research project, the research team applied a three-stage SPF calibration approach as follows:

1. Assemble a database of all available segments with each lane count (4, 6, 8, or 10 general-purpose lanes) and use these segments to calibrate the base SPFs without applying their corresponding CMFs.
2. Assemble a sample of up to 550 segments with each lane count and use these segments to calibrate the base SPFs with their CMFs that require data that is readily available in the state roadlog database (e.g., lane and shoulder width).
3. Assemble a sample of up to 50 segments with each lane count and use these segments to calibrate the base SPFs with all their CMFs, including those that require data from supplemental data sources (e.g., longitudinal barrier or rumble strip presence). Also use these segments to compute local calibration factors for the SDFs.

The research team queried several TxDOT-maintained databases that are essential to the calculation of local calibration factors. These databases included the TRM database, which is the state's roadlog database, and the CRIS database, which archives records of crashes on state-maintained roadways. The research team categorized the segments by lane count and type (i.e., general-purpose, auxiliary, or managed lanes). Managed lanes included HOV, HOT, and toll lanes. Table 14 provides the summary statistics for the urban freeway segments in Texas based on the TRM database query and review of aerial photographs, including segments with no auxiliary or managed lanes and with "typical" geometry. Segments that had general-purpose lanes and one or more managed lanes are listed as "*x*–*y* w/ML" in the first column of Table 14, where *x*–*y* is the range for the number of general-purpose lanes.

Table 15 provides the count of segments with managed lanes by lane counts. Most freeway segments with managed lanes have one or two managed lanes built as one reversible lane or one lane in each direction of travel.

**Table 14. Urban Freeway Segment Summary Statistics (All Segments).**

| Number of Lanes | Number of Segments | Variable Range | | | | | | |
|---|---|---|---|---|---|---|---|---|
| | | AADT, veh/day | Segment Length, mi | Crash Count by Type and Severity | | | | |
| | | | | MV-FI | MV-PDO | SV-FI | SV-PDO | Total |
| 4 | 785 | 2363–202,376 | 0.018–5.192 | 0–100 | 0–177 | 0–51 | 0–115 | 0–391 |
| 4 w/ML | 38 | 43,299–153,523 | 0.004–1.058 | 0–52 | 0–80 | 0–14 | 0–22 | 0–166 |
| 5–6 | 850 | 10,217–227,952 | 0.001–3.076 | 0–135 | 0–269 | 0–79 | 0–88 | 0–470 |
| 5–6 w/ML | 75 | 99,338–250,224 | 0.002–1.283 | 0–42 | 0–140 | 0–15 | 0–27 | 0–218 |
| 7–8 | 553 | 27,201–253,067 | 0.002–3.701 | 0–252 | 0–824 | 0–118 | 0–262 | 0–1456 |
| 7–8 w/ML | 253 | 99,338–314,266 | 0.001–2.392 | 0–297 | 0–602 | 0–92 | 0–111 | 0–967 |
| 9–10 | 188 | 44,278–267,936 | 0.001–2.266 | 0–438 | 0–1071 | 0–41 | 0–82 | 0–1565 |
| 9–10 w/ML | 131 | 99,338–314,266 | 0.001–3.621 | 0–447 | 0–1140 | 0–69 | 0–135 | 0–1764 |
| 11–12 | 24 | 168,142–267,131 | 0.006–0.611 | 0–107 | 0–249 | 0–11 | 0–28 | 0–391 |
| 11–12 w/ML | 24 | 164,375–330,096 | 0.011–1.386 | 0–219 | 0–509 | 0–31 | 0–103 | 0–862 |

**Table 15. Distribution of Segments by Lane Count (Segments with Managed Lanes).**

| Number of General-Purpose Lanes | Segment Count by Number of Managed Lanes | | | | | |
|---|---|---|---|---|---|---|
| | 1 | 2 | 3 | 4 | 6 | Total |
| 4 | 0 | 10 | 2 | 25 | 1 | 38 |
| 5 | 0 | 1 | 0 | 8 | 1 | 10 |
| 6 | 5 | 44 | 7 | 9 | 0 | 65 |
| 7 | 17 | 9 | 2 | 4 | 0 | 32 |
| 8 | 74 | 131 | 0 | 11 | 5 | 221 |
| 9 | 19 | 15 | 0 | 5 | 1 | 40 |
| 10 | 38 | 23 | 8 | 21 | 1 | 91 |
| 11 | 7 | 2 | 1 | 6 | 0 | 16 |
| 12 | 4 | 0 | 0 | 0 | 0 | 4 |
| 13 | 1 | 0 | 2 | 1 | 0 | 4 |
| Total | 165 | 235 | 22 | 90 | 9 | 521 |

Table 16 provides the distribution of managed-lane segment characteristics, including the buffer type and the presence or absence of reversible operations. The bulk of the segments have barriers to separate the managed lane(s) from the adjacent general-purpose lanes.

**Table 16. Managed-Lane Segment Count.**

| Number of General-Purpose Lanes (one-way total) | Buffer Type | | | Reversible? | | Total |
|---|---|---|---|---|---|---|
| | **Barrier** | **Stripe** | **Pylons** | **No** | **Yes** | |
| 1 | 162 | 2 | 1 | 14 | 151 | 165 |
| 2 | 124 | 61 | 50 | 162 | 73 | 235 |
| 3 | 11 | 0 | 11 | 22 | 0 | 22 |
| 4 | 71 | 0 | 19 | 82 | 8 | 90 |
| 6 | 8 | 0 | 1 | 9 | 0 | 9 |
| **Total** | 376 | 63 | 82 | 289 | 232 | 521 |

The research team used the Stage 3 dataset to compute SDF calibration factors. The SDF calibration procedure is described in detail in Appendix B of the HSM and summarized by Equations 15–17:

$$P_{o,KAB} = \frac{N_{o,KAB}}{N_{o,KABC}} \tag{15}$$

$$P_{p,KAB} = \frac{N_{p,KAB}}{N_{p,KABC}} \tag{16}$$

$$C_{SDF} = \frac{P_{o,KAB}}{1 - P_{o,KAB}} \times \frac{1 - P_{p,KAB}}{P_{p,KABC}} \tag{17}$$

where:

$N_{o\_KABC}$ = observed number of KABC crashes;
$N_{o\_KAB}$ = observed number of KAB crashes;
$N_{p\_KABC}$ = predicted number of KABC crashes;
$N_{p\_KAB}$ = predicted number of KAB crashes;
$P_{o,KAB}$ = observed probability of a severe crash;
$P_{p,KAB}$ = predicted probability of a severe crash; and
$C_{SDF}$ = SDF local calibration factor.

**Calculation Results**

To compute calibration factors, the research team used the segments without managed lanes as grouped by lane count in Table 14. The research team included segments with odd-numbered lane counts to obtain a small increase in the sample size for each category.

Table 17 provides the results of the Stage 1 calibration factor analysis for the SPFs. As previously stated, this stage included the exposure variables (i.e., traffic volume and segment length); however, the research team also included rumble strip presence data and applied the rumble strip CMFs. These calibration factors suggest that the HSM SPFs for multiple-vehicle crashes on 10-lane segments are a poor fit for Texas segments (i.e., *C* values greater than 2.0).

Table 18 provides the results of the Stage 2 calibration factor analysis. This stage included the exposure variables, geometric variables available in the TRM database (e.g., cross-sectional widths), variables to describe rumble strip presence, Type B weaving section presence

and length, and horizontal curve presence and length.  The Stage 2 calibration factors were not notably different from the Stage 1 calibration factors.

**Table 17.  Local Calibration Factors—Stage 1 Results.**

| Number of Lanes | Crash Type and Severity | Crash Count | | Local SPF Calibration Factor $C$ |
| --- | --- | --- | --- | --- |
| | | Observed | Predicted | |
| 4 | SV-FI | 1446 | 1796.94 | 0.80 |
| | SV-PDO | 3167 | 3357.84 | 0.94 |
| | MV-FI | 2159 | 2076.58 | 1.04 |
| | MV-PDO | 4613 | 4383.76 | 1.05 |
| 5–6 | SV-FI | 2666 | 3082.97 | 0.86 |
| | SV-PDO | 4765 | 5586.35 | 0.85 |
| | MV-FI | 6229 | 5155.07 | 1.21 |
| | MV-PDO | 13,048 | 11,638.68 | 1.12 |
| 7–8 | SV-FI | 2355 | 2361.75 | 1.00 |
| | SV-PDO | 3923 | 3935.55 | 1.00 |
| | MV-FI | 7980 | 5551.74 | 1.44 |
| | MV-PDO | 15,667 | 13,022.45 | 1.20 |
| 9–10 | SV-FI | 672 | 682.68 | 0.98 |
| | SV-PDO | 1278 | 1079.68 | 1.18 |
| | MV-FI | 3087 | 1416.03 | 2.18 |
| | MV-PDO | 7303 | 3413.51 | 2.14 |

**Table 18.  Local Calibration Factors—Stage 2 Results.**

| Number of Lanes | Crash Type and Severity | Crash Count | | Local SPF Calibration Factor $C$ |
| --- | --- | --- | --- | --- |
| | | Observed | Predicted | |
| 4 | SV-FI | 752 | 1025.14 | 0.73 |
| | SV-PDO | 1635 | 1955.48 | 0.84 |
| | MV-FI | 1047 | 1109.9 | 0.94 |
| | MV-PDO | 2255 | 2270.67 | 0.99 |
| 5–6 | SV-FI | 1625 | 1798.31 | 0.90 |
| | SV-PDO | 2736 | 3414.45 | 0.80 |
| | MV-FI | 3573 | 2990.55 | 1.19 |
| | MV-PDO | 7060 | 6672.2 | 1.06 |
| 7–8 | SV-FI | 1598 | 1525.71 | 1.05 |
| | SV-PDO | 2544 | 2717.79 | 0.94 |
| | MV-FI | 5219 | 3807.46 | 1.37 |
| | MV-PDO | 10,230 | 8938.12 | 1.14 |
| 9–10 | SV-FI | 578 | 593.20 | 0.97 |
| | SV-PDO | 1121 | 960.48 | 1.17 |
| | MV-FI | 2862 | 1279.16 | 2.24 |
| | MV-PDO | 6783 | 3101.64 | 2.19 |

Table 19 provides the results of the Stage 3 calibration factor analysis.  This stage included all previously-used variables (i.e., exposure variables, geometric variables available in the TRM database, rumble strip presence, Type B weaving section presence and length, and horizontal curve presence and length) plus variables to describe the following characteristics: continuous median barrier presence and type; length and offset of roadside and short median

barrier pieces; clear zone width; and entrance and exit ramp presence, location, and volume. Once all these additional variables were included in the calibration analysis, all the calibration factors were found to be within the range of 0.5–1.5. In particular, the factors for multiple-vehicle FI and PDO crashes on 10-lane segments decreased to 1.41 and 1.30, respectively, suggesting that the inclusion of the variables needed to compute the lane change CMF value resulted in a notable improvement in the model quality.

**Table 19. Local Calibration Factors—Stage 3 Results.**

| Number of Lanes | Crash Type and Severity | Crash Count | | Local SPF Calibration Factor $C$ |
|---|---|---|---|---|
| | | Observed | Predicted | |
| 4 | SV-FI | 74 | 95.68 | 0.77 |
| | SV-PDO | 144 | 211.71 | 0.68 |
| | MV-FI | 96 | 148.55 | 0.65 |
| | MV-PDO | 178 | 312.02 | 0.57 |
| 5–6 | SV-FI | 137 | 194.74 | 0.70 |
| | SV-PDO | 214 | 384.55 | 0.56 |
| | MV-FI | 449 | 474.14 | 0.95 |
| | MV-PDO | 785 | 1104.81 | 0.71 |
| 7–8 | SV-FI | 305 | 244.94 | 1.25 |
| | SV-PDO | 507 | 487.12 | 1.04 |
| | MV-FI | 935 | 735.81 | 1.27 |
| | MV-PDO | 2083 | 1734.36 | 1.20 |
| 9–10 | SV-FI | 93 | 91.49 | 1.02 |
| | SV-PDO | 156 | 164.88 | 0.95 |
| | MV-FI | 368 | 260.63 | 1.41 |
| | MV-PDO | 833 | 638.66 | 1.30 |

## Evaluation of Calibration Factor Quality

To evaluate the quality of calibration factors, various goodness-of-fit measures were used, as described below. These measures included cumulative residual plots, error-based methods, dispersion parameters, and coefficients of variation.

*Cumulative Residual Plot*

A CURE plot is a graph of cumulative residuals (i.e., observed crashes minus predicted crashes) plotted against a variable of interest in ascending order. The variable of interest is often AADT or predicted crashes. The visual presentation of a CURE plot shows the concerning areas that may require improvement of SPFs such as percent areas increasing confidence limits, long trends, and vertical changes (*41*).

The CURE plots for each segment type are constructed using the following steps.

1. The variables of interest are sorted in ascending order.
2. For each site, the residual is calculated as the difference between observed and predicted crashes.
3. The cumulative of residuals is then calculated as the sum of residuals 1 to *n*, where *n* is the total number of sites.

36

4. The square of residuals is calculated, followed by the calculation of cumulative squared residuals.
5. The 95-percent confidence interval (*CI*) limits are then calculated for each site:

$$CI = \pm 1.96\sqrt{\sigma^2} \tag{18}$$

where:

$\sigma^2$  =  the variance of the random walk.

*Error-Based Methods*

Two error-based methods are used to analyze goodness of fit (*33, 41*). These methods include MAD, which calculates the absolute difference between the predicted number of crashes and observed number of crashes, and mean squared prediction error (MSPE), which calculates the square of the difference between the predicted and observed number of crashes. These methods are described by the following equations:

$$MAD = \frac{1}{n}\sum_{i=1}^{n}|\mu_i - y_i| \tag{19}$$

$$MSPE = \frac{1}{n}\sum_{i=1}^{n}(\mu_i - y_i)^2 \tag{20}$$

*Dispersion Parameter*

A dispersion parameter (*k*) shows the spread of observed crashes about predicted value of crashes. Since the SPFs were recalibrated, the dispersion parameter also needed to be recalibrated. The dispersion parameter was estimated for the recalibrated SPFs using the weighted regression analysis proposed by Cameron and Trivedi (*42*). By forcing the intercept to be zero, a straight line was fitted as follows:

$$Y = k \times \mu_i{}^2 \tag{21}$$

with:

$$Y = (y_i - \mu_i)^2 - y_i \tag{22}$$

*Coefficient of Variation of Calibration Factor*

The coefficient of variation (*CV*) is calculated as the standard deviation of the calibration factor divided by the predicted calibration factor as follows:

$$CV = \frac{\sqrt{V(C)}}{C} \tag{23}$$

with:

$$V(C) = \frac{\sum_i (y_i + k y_i^2)}{\left(\sum_i \hat{y}_i\right)^2}$$ (24)

where:

$V(C)$ = variance of the calibration factor;

$\hat{y}_i$ = uncalibrated predicted annual crash frequency for site $i$; and

$k$ = recalibrated dispersion parameter.

An SPF is deemed to be acceptable when one of the following conditions is true (*41*):

- Five percent or less of CURE plot ordinates for the calibrated predicted values exceed the $2\sigma$ limits.
- The *CV* of the calibration factor is less than 0.15.

*Evaluation Results*

Table 20 summarizes the calibration factors by the number of freeway lanes. The results show that the calibration factors vary from 0.56 to 1.41.

**Table 20. Calibration Factors, Tabular Format.**

| No. of Lanes | Crash Type and Severity | Local SPF Calibration Factor *C* | Standard Error |
|---|---|---|---|
| 4 | SV-FI | 0.77 | 0.12 |
| | SV-PDO | 0.68 | 0.14 |
| | MV-FI | 0.65 | 0.13 |
| | MV-PDO | 0.57 | 0.12 |
| 6 | SV-FI | 0.70 | 0.10 |
| | SV-PDO | 0.56 | 0.08 |
| | MV-FI | 0.95 | 0.10 |
| | MV-PDO | 0.71 | 0.08 |
| 8 | SV-FI | 1.25 | 0.13 |
| | SV-PDO | 1.04 | 0.11 |
| | MV-FI | 1.27 | 0.11 |
| | MV-PDO | 1.20 | 0.09 |
| 10 | SV-FI | 1.02 | 0.13 |
| | SV-PDO | 0.95 | 0.11 |
| | MV-FI | 1.41 | 0.09 |
| | MV-PDO | 1.30 | 0.07 |
| 4–10 | SV-FI | 1.02 | 0.08 |
| | SV-PDO | 0.95 | 0.06 |
| | MV-FI | 1.41 | 0.07 |
| | MV-PDO | 1.30 | 0.07 |

The factors are also shown in graphical format in Figure 16. The *x*-axis gridline for a factor value of 1.0 is shown as a green line to denote the ideal case of an HSM model's predictions exactly matching the observed crashes in Texas. The factors from the fourth column of Table 20 are shown as blue bars, and the standard error ranges from the fifth column of Table 20 are shown as red bars. Note the following observations:

- Two of the four calibration factors for 4–10 lanes shown on the bottom portion of Figure 16 are close to 1.0, indicating that the HSM models closely matched Texas conditions. These models are for SV-FI crashes and MV-PDO crashes. Conversely, the SV-PDO model notably under-predicts for Texas, and the MV-FI model slightly over-predicts for Texas.
- The calibration factors for smaller lane counts (4 or 6 lanes) are lower than 1.0, suggesting that the HSM models for these lane counts over-predict for Texas conditions.
- The calibration factors for larger lane counts (8 or 10 lanes) are higher than 1.0, suggesting that the HSM models for these lane counts under-predict for Texas conditions.
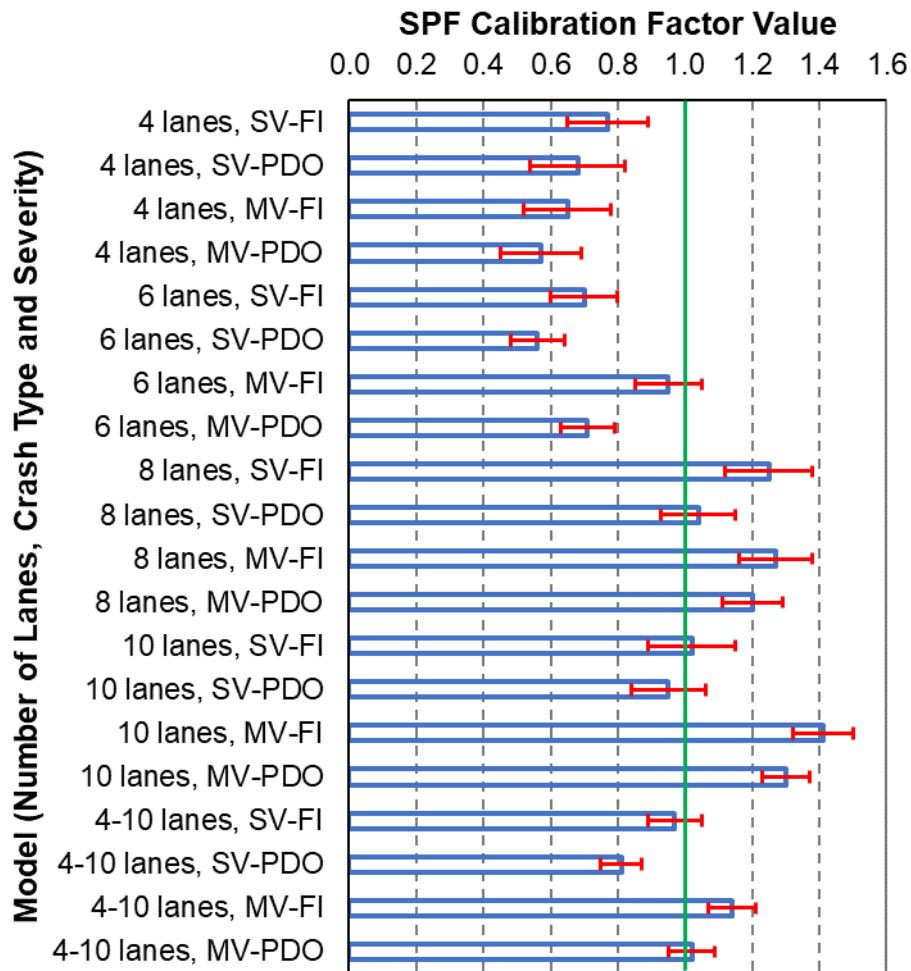


**Figure 16. Calibration Factors, Graphical Format.**

The following figures show plots for the various combinations of lane count, crash type, and crash severity:

- Figure 17.  CURE Plots for Crashes on 4-Lane Freeways.
- Figure 18.  CURE Plots for Crashes on 6-Lane Freeways.
- Figure 19.  CURE Plots for Crashes on 8-Lane Freeways.
- Figure 20.  CURE Plots for Crashes on 10-Lane Freeways.
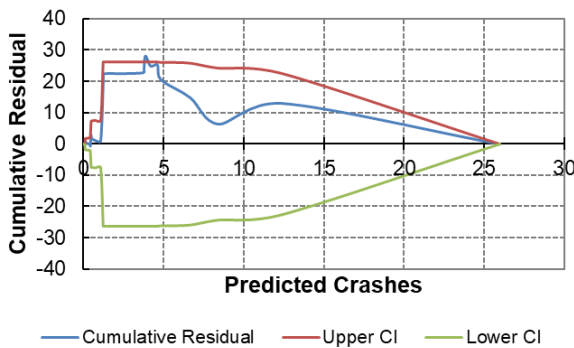- Figure 21.  CURE Plots for Crashes on 4-10-Lane Freeways.

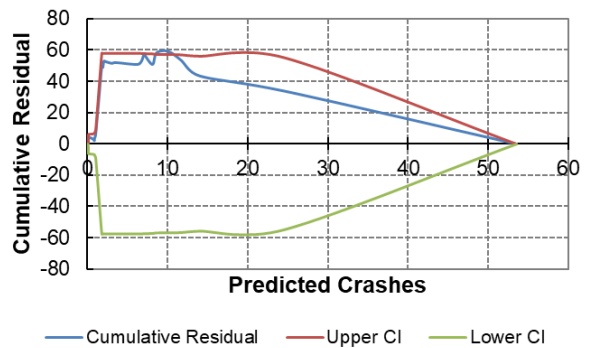The figures show that, except for a few sites, the re-calibrated models predict crashes accurately.
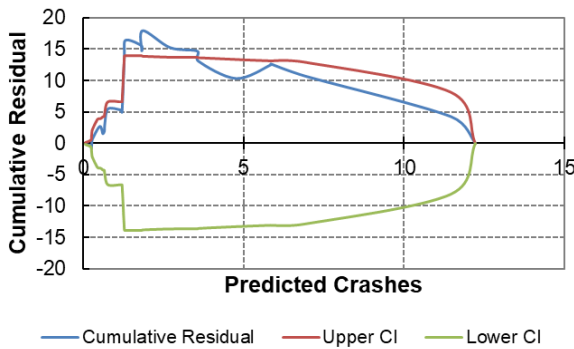
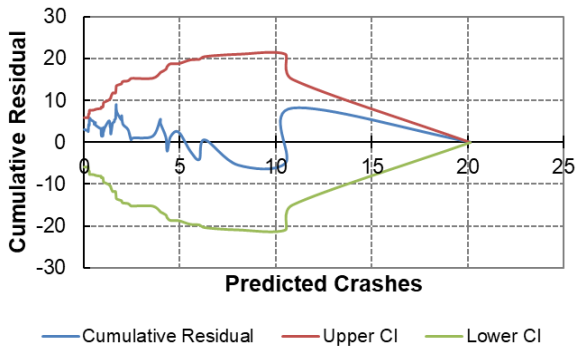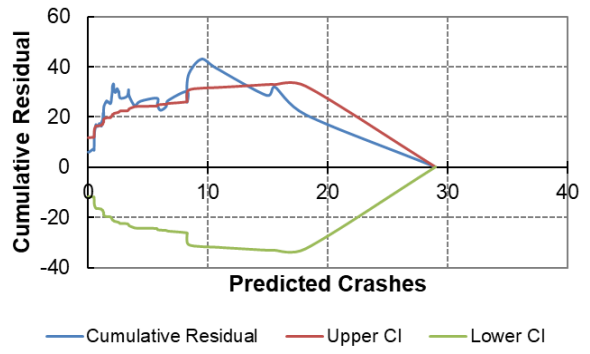

a.  SV-FI Crashes
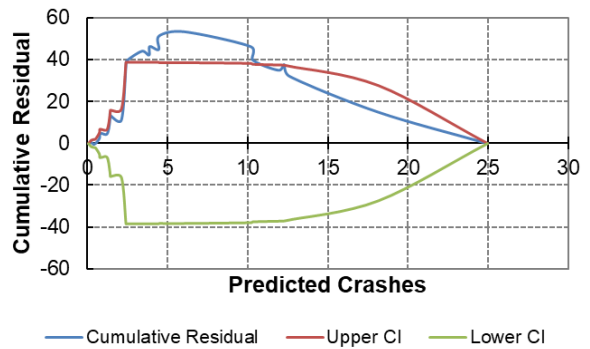
b.  SV-PDO Crashes

c.  MV-FI Crashes

b.  MV-PDO Crashes

**Figure 17.  CURE Plots for Crashes on 4-Lane Freeways.**

a. SV-FI Crashes

b. SV-PDO Crashes

c. MV-FI Crashes

b. MV-PDO Crashes

**Figure 18. CURE Plots for Crashes on 6-Lane Freeways.**



a. SV-FI Crashes

b. SV-PDO Crashes

c. MV-FI Crashes

b. MV-PDO Crashes

**Figure 19. CURE Plots for Crashes on 8-Lane Freeways.**
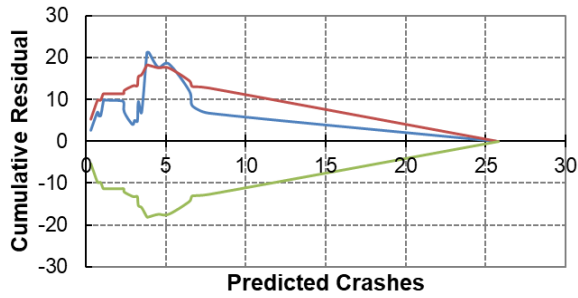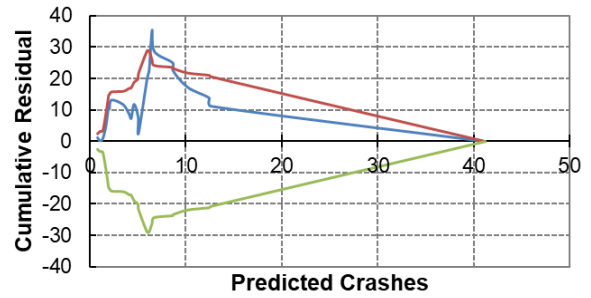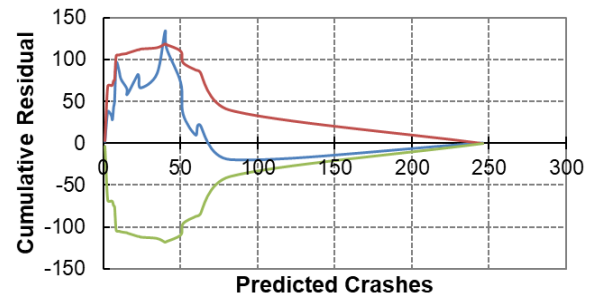
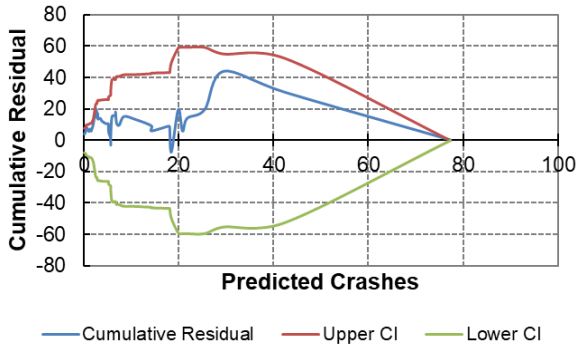a. SV-FI Crashes

b. SV-PDO Crashes

c. MV-FI Crashes

b. MV-PDO Crashes

**Figure 20. CURE Plots for Crashes on 10-Lane Freeways.**
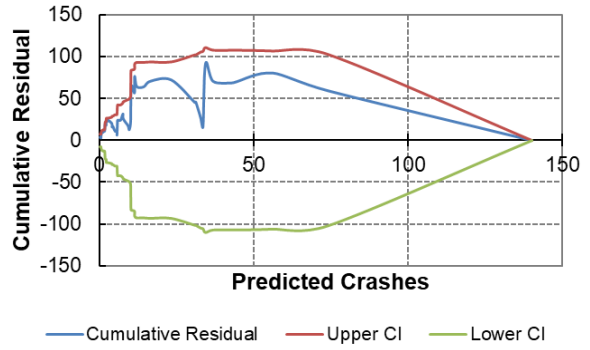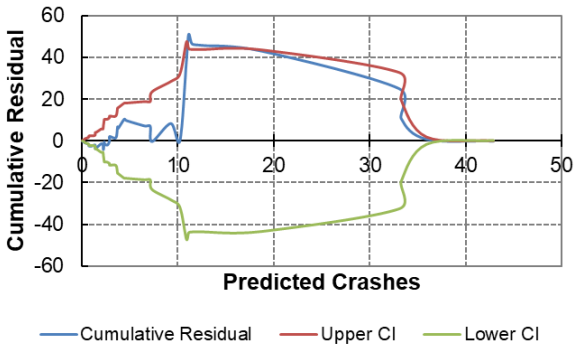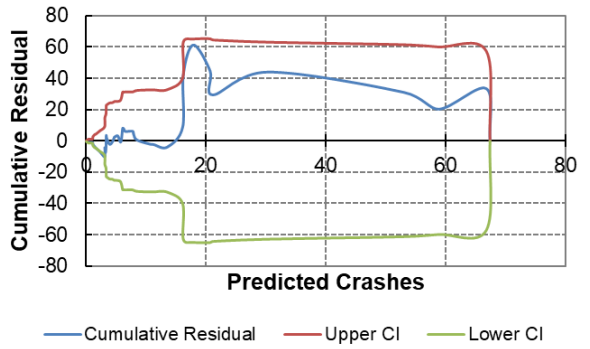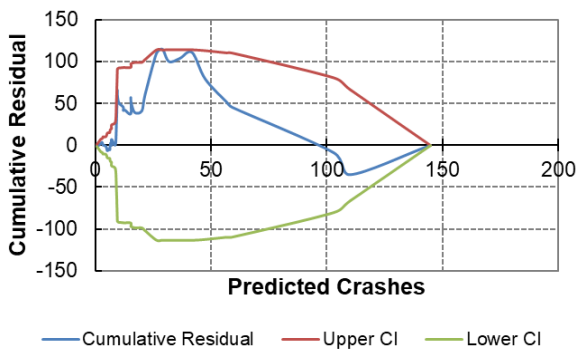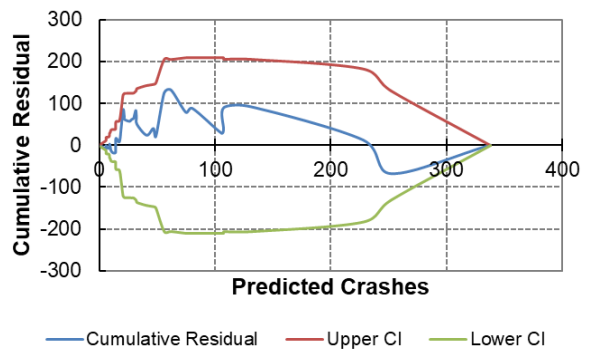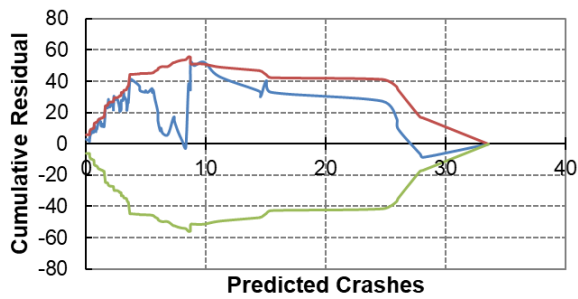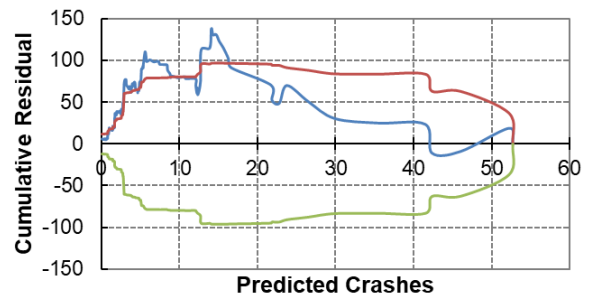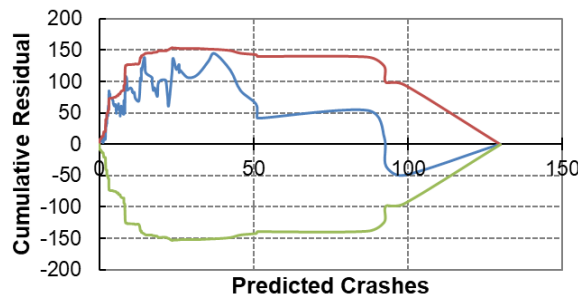


a. SV-FI Crashes

b. SV-PDO Crashes

c. MV-FI Crashes
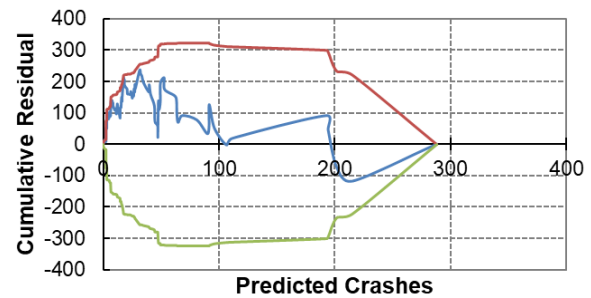
b. MV-PDO Crashes

**Figure 21. CURE Plots for Crashes on 4-10-Lane Freeways.**

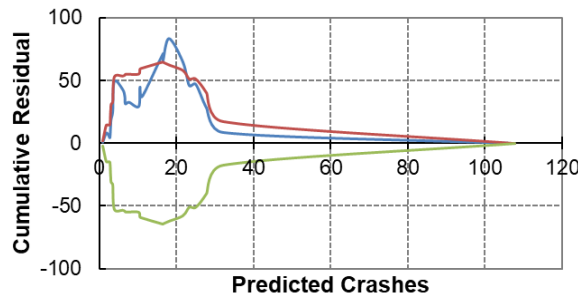Table 21 shows the results for the different goodness-of-fit measures, as described above. The table reports the values for MAD, MSPE, re-calibrated dispersion parameter, and percentage of the CURE plot lines that fall beyond the 95-percent confidence intervals. Except for three SPFs, the CV is within 0.15 for all SPFs, which shows that the calibrated SPFs can accurately estimate crashes in Texas. Out of those three SPFs whose CV values are greater than 0.15, two of them exceed 6 percent or less of CURE plot ordinates for calibrated predicted values. This means those calibrated SPFs can accurately estimate crashes. Note that models for SV-PDO crashes tend to have the largest percent of CURE plot exceeding the 95-percent confidence intervals. These crashes tend to be the least common crash types on urban freeways. The trend with the CURE plots for these crashes may be due to differences in crash reporting practices for these types of crashes between Texas and the states originally used to calibrate the HSM models (i.e., Washington, California, and Maine).

### Table 21. Goodness-of-Fit Measures for the Re-Calibrated Models.

| No. of Lanes | Crash Type and Severity | Calibration Factor | MAD | MSPE | Overdispersion Parameter | CV | Exceeding 95% CI |
|---|---|---|---|---|---|---|---|
| 4 | SV-FI | 0.77 | 1.57 | 6.21 | 0.14 | 0.15 | 19% |
| | SV-PDO | 0.68 | 4.15 | 48.20 | 0.42 | 0.20 | 32% |
| | MV-FI | 0.65 | 2.49 | 22.32 | 0.24 | 0.20 | 3% |
| | MV-PDO | 0.57 | 4.59 | 108.94 | 0.37 | 0.22 | 6% |
| 6 | SV-FI | 0.70 | 1.89 | 8.87 | 0.21 | 0.15 | 0% |
| | SV-PDO | 0.56 | 3.00 | 21.86 | 0.45 | 0.15 | 64% |
| | MV-FI | 0.95 | 4.92 | 70.32 | 0.16 | 0.11 | 0% |
| | MV-PDO | 0.71 | 8.94 | 279.14 | 0.18 | 0.11 | 0% |
| 8 | SV-FI | 1.25 | 4.11 | 65.74 | 0.10 | 0.10 | 8% |
| | SV-PDO | 1.04 | 6.39 | 109.11 | 0.11 | 0.11 | 8% |
| | MV-FI | 1.27 | 11.65 | 334.01 | 0.09 | 0.11 | 3% |
| | MV-PDO | 1.20 | 21.77 | 1138.65 | 0.07 | 0.07 | 0% |
| 10 | SV-FI | 1.02 | 2.75 | 17.29 | 0.05 | 0.13 | 17% |
| | SV-PDO | 0.95 | 4.53 | 36.24 | 0.06 | 0.11 | 13% |
| | MV-FI | 1.41 | 10.54 | 184.08 | 0.01 | 0.06 | 17% |
| | MV-PDO | 1.30 | 19.90 | 612.58 | 0.01 | 0.05 | 4% |
| 4–10 | SV-FI | 0.97 | 2.63 | 25.82 | 0.17 | 0.08 | 7% |
| | SV-PDO | 0.81 | 4.49 | 64.09 | 0.21 | 0.08 | 60% |
| | MV-FI | 1.14 | 7.38 | 162.01 | 0.13 | 0.07 | 7% |
| | MV-PDO | 1.02 | 15.47 | 719.17 | 0.16 | 0.07 | 0% |

Figure 22 shows a graphical comparison of the calibrated SPFs for urban freeways with 4–6 general-purpose lanes. These SPFs show that for a given traffic volume, SV-FI crash frequency and PDO crash frequency will decrease slightly as the number of lanes increases from four to six, while MV-FI crash frequency will increase slightly. In all cases, the magnitudes of the changes in crash frequency are small. For example, at a traffic volume of 100,000 veh/day, the difference in MV-FI crash frequency between a six-lane segment and a four-lane segment is about one crash per mile per year.
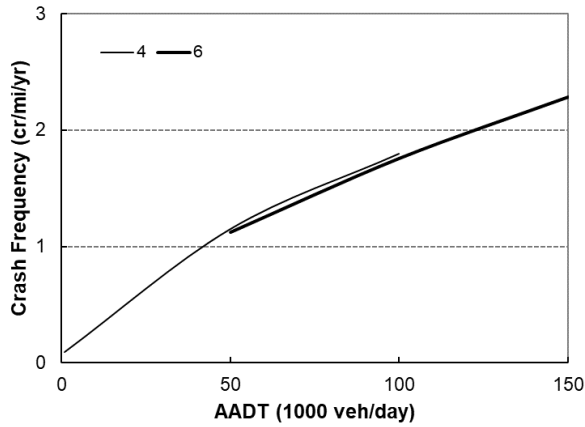
a. SV-FI Crashes
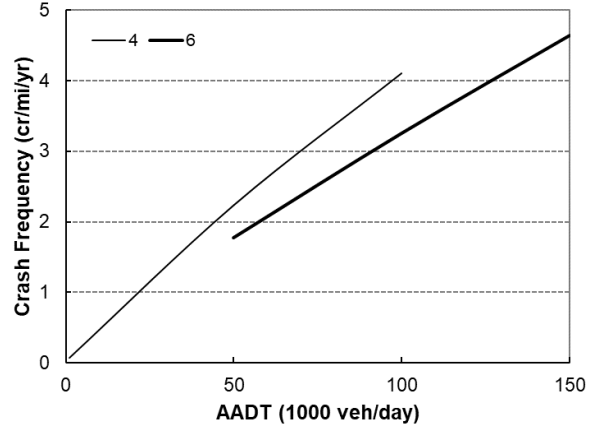


b. SV-PDO Crashes
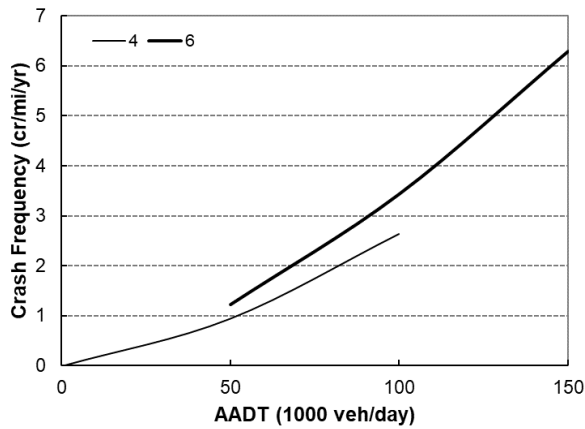


c. MV-FI Crashes
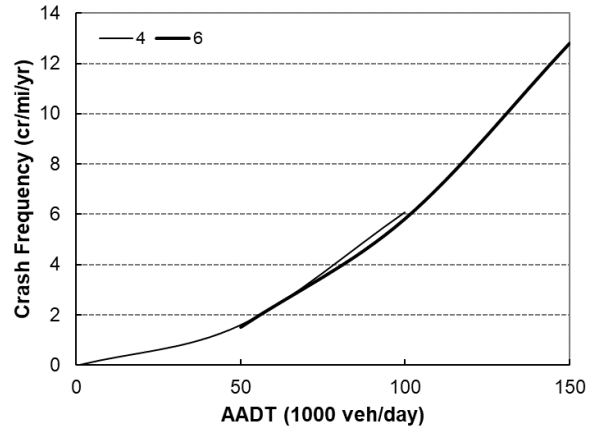


d. MV-PDO Crashes

**Figure 22. Calibrated SPFs for Urban Freeways with 4–6 Lanes.**

The research team used the Stage 2 data to apply the 10-lane freeway models to freeways with 12 lanes. Table 22 provides the model coefficients and goodness-of-fit measures. Figure 23 shows CURE plots for crashes on 12-lane freeways. These plots show that the re-calibrated model predicts crashes accurately.

**Table 22. Goodness-of-Fit Measures for Re-Calibrated Models for 12-Lane Freeways.**

| Crash Type and Severity | Local SPF Calibration Factor | MAD | MSPE | Overdispersion Parameter | CV | Exceeding 95% CI |
|---|---|---|---|---|---|---|
| SV-FI | 1.01 | 1.56 | 4.83 | 0.09 | 0.11 | 0% |
| SV-PDO | 0.77 | 1.71 | 4.77 | 0.03 | 0.15 | 4% |
| MV-FI | 1.13 | 2.32 | 10.12 | 0.02 | 0.08 | 4% |
| MV-PDO | 1.04 | 4.93 | 40.14 | 0.01 | 0.06 | 0% |

**a. SV-FI Crashes**

**b. SV-PDO Crashes**

**c. MV-FI Crashes**

**b. MV-PDO Crashes**
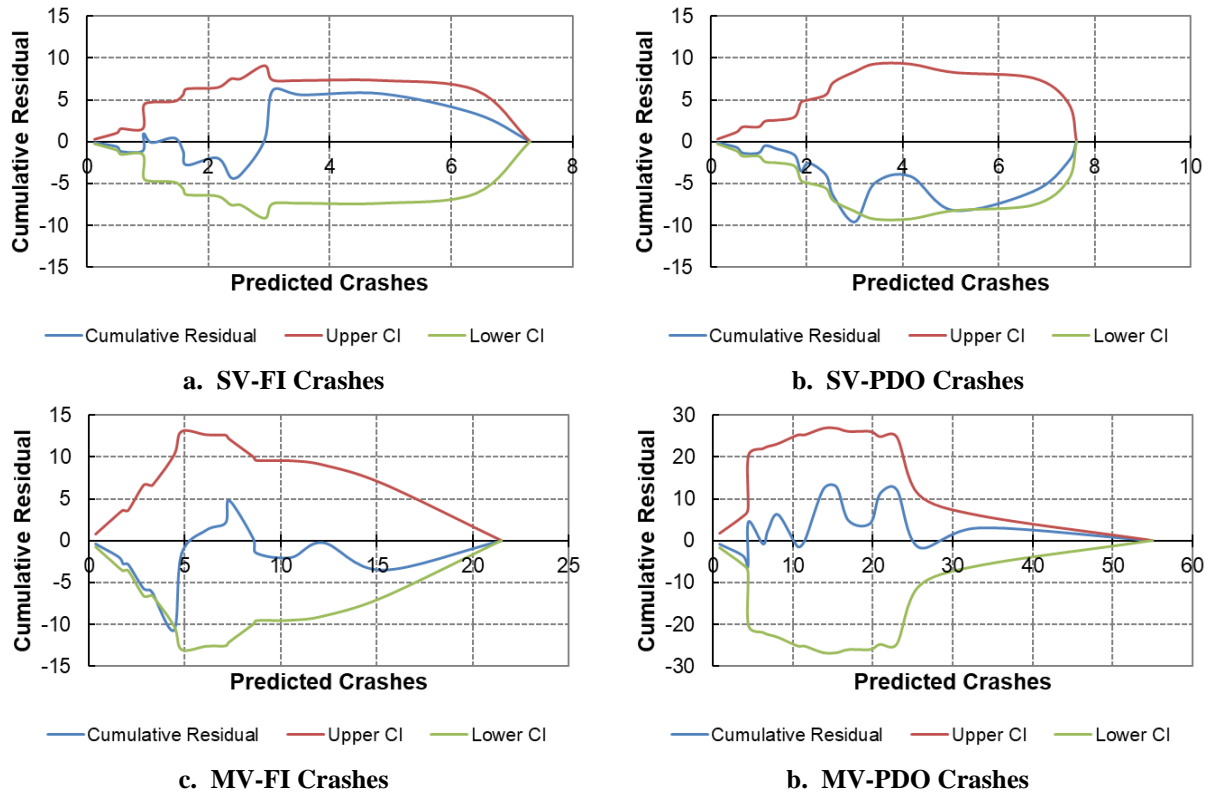
**Figure 23. CURE Plots for Crashes on 12-Lane Freeways.**

Figure 24 shows a graphical comparison of the calibrated SPFs for urban freeways with 8–12 general-purpose lanes. These SPFs show that for a given traffic volume, crash frequency will decrease as the number of lanes increases. This trend is consistent with the SPFs for segments with 4–10 lanes, reported in the *Workbook* (*1*) and the HSM (*2*) without local calibration and extending to segments with more than 10 lanes. However, when the trend for 8-lane segments is compared with the trend for 6-lane segments, a notable increase in crash frequency is observed as the lane count increases. This trend may be due to differences in land development and area type. Segments with 4–6 lanes tend to be located in areas that are classified as urban but tend to be smaller in population and population density (e.g., suburban or exurban), while segments with 8–12 lanes tend to be located in urbanized or metropolitan areas that have a higher and denser population.

Table 23 provides the observed and predicted number of crashes, observed and predicted probability of severe crashes, and SDF local calibration factor by number of lanes. The calibration factors are in the bottom row of the table. For every lane count and for the overall dataset, the observed probability of a severe crash was higher than the predicted probability of a severe crash.

The research team used the Stage 3 dataset to compute the SDF local calibration factors because the SDFs account for longitudinal barrier presence (among other variables), and the variables to account for longitudinal barriers were only available in the Stage 3 dataset. Since the sample size (in terms of number of segments) was so small for segments with 12 lanes, the research team could not directly compute an SDF local calibration factor for these segments.

45

Instead, the research team recommends applying the SDF local calibration factor for segments with 10 lanes to the SDF for segments with 12 lanes.
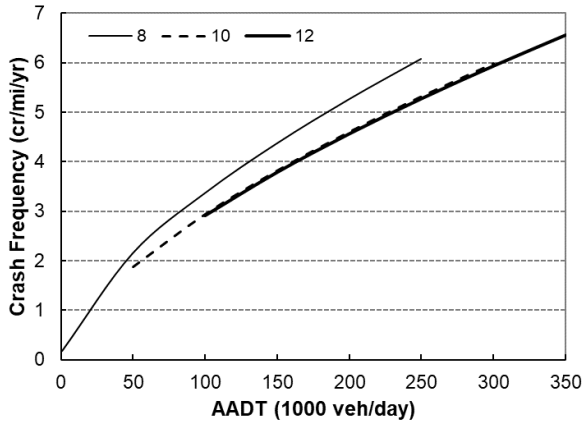


a. SV-FI Crashes
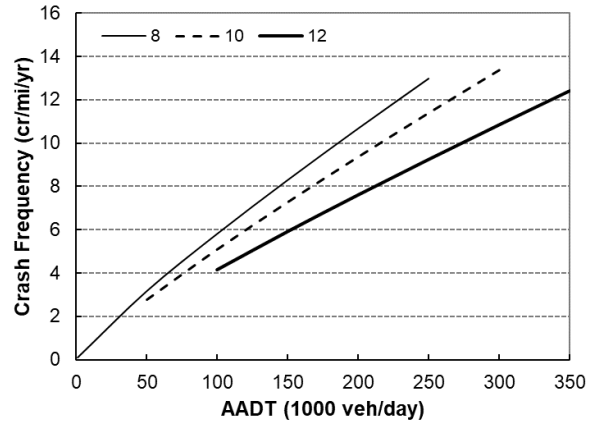
b. SV-PDO Crashes
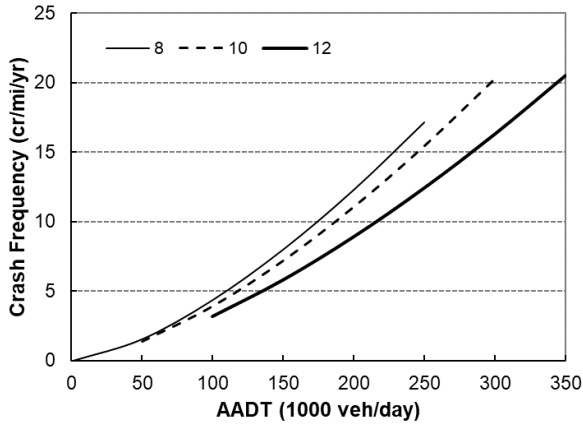
c. MV-FI Crashes
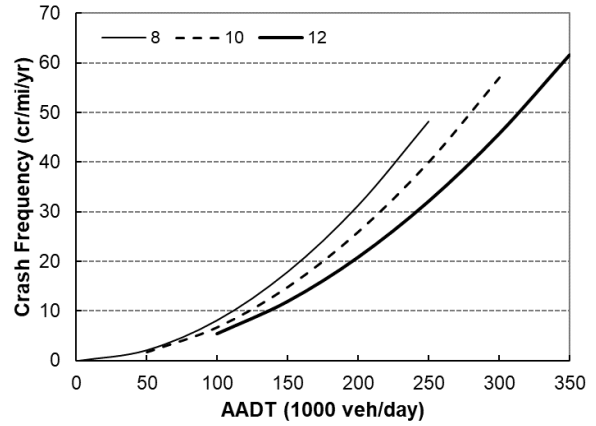
d. MV-PDO Crashes

**Figure 24. Calibrated SPFs for Urban Freeways with 8–12 Lanes.**

**Table 23. SDF Calibration Results.**

| Variable | Variable Value by Number of Lanes | | | | |
|---|---|---|---|---|---|
| | **4** | **5–6** | **7–8** | **9–10** | **4–10** |
| $N_{o\_KABC}$ | 186 | 668 | 1444 | 572 | 2870 |
| $N_{o\_KAB}$ | 100 | 293 | 555 | 226 | 1174 |
| $N_{p\_KABC}$ | 244.23 | 668.88 | 980.74 | 371.07 | 2264.92 |
| $N_{p\_KAB}$ | 84.93 | 197.59 | 270.13 | 98.97 | 651.62 |
| $P_{o,KAB}$ | 0.54 | 0.44 | 0.38 | 0.40 | 0.41 |
| $P_{p,KAB}$ | 0.35 | 0.30 | 0.28 | 0.27 | 0.29 |
| $C_{SDF}$ | 2.18 | 1.86 | 1.64 | 1.80 | 1.71 |

## CALIBRATION OF MODELS FOR URBAN MANAGED-LANE FACILITIES

The research team calibrated new safety prediction models for managed-lane facilities on urban freeway segments. These models apply to crashes inside or involving the managed lanes, including crashes at access points where ramps or weaving sections connect the managed lanes to the adjacent general-purpose lanes or other roadways. The previously documented models and local calibration factors are used to predict crash frequency in the general-purpose lanes.

The new models apply to managed lanes that are separated from the adjacent general-purpose lanes by the following buffer types:

- Barrier—longitudinal positive barriers, typically concrete.
- Pylons—a continuous row of plastic pylons.
- Stripe—pavement markings, typically two solid white lines.

The research team calibrated one set of models for non-reversible managed lanes, which can be separated from the adjacent general-purpose lanes using any of the listed buffer types, and an additional model for reversible managed lanes, which are separated from general-purpose lanes using barriers and are typically located in the median. These models account for the safety effect of key geometric variables, including inside and outside shoulder width and access point density. Access point density accounts for the number and type of access points, differentiating between weaving sections and ramps.

### Model Functional Form

The predictive model calibration process consisted of simultaneous calibration of multiple-vehicle and single-vehicle crash models and CMFs using an aggregate model. The simultaneous calibration approach was needed because several CMFs are common to multiple-vehicle and single-vehicle crash models. The database assembled for calibration included two replications of the original database. The dependent variable in the first replication was set equal to the multiple-vehicle crash count. The dependent variable in the second replication was set equal to the single-vehicle crash count. The predicted average crash frequency in the managed lanes of a freeway was calculated as follows:

$$N_{i,j} = (N_{i,sv}I_{i,sv} + N_{i,mv}I_{i,mv}) \tag{25}$$

where:

$N_{i,j}$ = predicted annual crash frequency for configuration $i$ (buffer type = barrier, pylons, or pavement stripes; operation = non-reversible or reversible) and crash type $j$ (single-vehicle or multiple-vehicle);

$N_{i,sv}$ = predicted annual single-vehicle crash frequency for configuration $i$;

$I_{i,sv}$ = indicator variable for single-vehicle crashes and configuration $i$ (= 1.0 for single-vehicle crash data, 0.0 otherwise);

$N_{i,mv}$ = predicted annual multiple-vehicle crash frequency for configuration $i$; and

$I_{i,mv}$ = indicator variable for multiple-vehicle crashes and configuration $i$ (= 1.0 for multiple-vehicle crash data, 0.0 otherwise).

For non-reversible managed lanes with barrier or pylon buffers, the predicted annual single- and multiple-vehicle crash frequencies were calculated as follows:

$$N_{sv} = N_{spf,sv} CMF_{is,sv} CMF_{ramp} \tag{26}$$

$$N_{mv} = N_{spf,mv} CMF_{os,mv} CMF_{wev} CMF_{ramp} \tag{27}$$

with:

$$N_{spf,sv} = L \, e^{b_{sv,0}+b_{sv,1}\ln(AADT)} \tag{28}$$

$$N_{spf,mv} = L \, e^{b_{mv,0}+b_{mv,1}\ln(AADT)} \tag{29}$$

$$CMF_{is,sv} = e^{b_{is,sv}(W_{is}-4)} \tag{30}$$

$$CMF_{os,mv} = e^{b_{os,mv}(W_{os}-4)} \tag{31}$$

$$CMF_{wev} = e^{(b_{wev}[n_{wev}/L])} \tag{32}$$

$$CMF_{ramp} = e^{(b_{ramp}[n_{ramp}/L])} \tag{33}$$

where:

$N_{spf,sv}$ = base predicted annual single-vehicle crash frequency, cr/yr;
$N_{spf,mv}$ = base predicted annual multiple-vehicle crash frequency, cr/yr;
$CMF_{is,sv}$ = inside shoulder width CMF for single-vehicle crashes;
$CMF_{os,mv}$ = outside shoulder width CMF for multiple-vehicle crashes;
$CMF_{wev}$ = access weaving section density CMF;
$CMF_{ramp}$ = access ramp density CMF;
$L$ = segment length, mi;
$AADT$ = annual average daily traffic in the managed lanes, veh/day;
$W_{is}$ = inside shoulder width, ft;
$W_{os}$ = outside shoulder width, ft;
$n_{wev}$ = number of access weaving sections in the managed lanes (the weaving section may extend beyond the segment endpoints);
$n_{ramp}$ = number of access ramp gores in the managed lanes (not including ramp gores connected to weaving sections in the managed lanes, as shown in Figure 15); and
$b_i$ = calibration coefficient for variable $i$.

For non-reversible managed lanes with striped buffers, the predicted annual single- and multiple-vehicle crash frequencies were calculated as follows:

$$N_{sv} = N_{spf,sv} CMF_{is,sv} \tag{34}$$

$$N_{mv} = N_{spf,mv} CMF_{os,mv} \tag{35}$$

For reversible managed lanes, the predicted annual single- and multiple-vehicle crash frequencies were calculated as follows:

$$N_{sv} = N_{spf,sv} CMF_{nl,sv} CMF_{ramp} \tag{36}$$

$$N_{mv} = N_{spf,mv} CMF_{nl,mv} CMF_{s,mv} CMF_{ramp} \tag{37}$$

with:

$$CMF_{nl,j} = e^{b_{nl,j} I_{nl}} \tag{38}$$

$$CMF_{s,mv} = e^{b_{s,mv}(W_s - 2)} \tag{39}$$

where:

$CMF_{nl,j}$ = number of lanes CMF for crash type $j$ (single-vehicle or multiple-vehicle);

$CMF_{s,mv}$ = shoulder width CMF for multiple-vehicle crashes;

$I_{nl}$ = indicator variable for number of lanes (= 1.0 if number of lanes is 2 or more, 0.0 otherwise); and

$W_s$ = average shoulder width, ft.

## Calibration Results

The following subsections provide the results of the model calibration for non-reversible and reversible managed lanes on urban freeways.

*Non-Reversible Lanes*

Table 24 contains the calibrated coefficients for non-reversible managed lanes. The SPF coefficients $b_{sv,0}$, $b_{mv,0}$, $b_{sv,1}$, and $b_{mv,1}$ show that for both single-vehicle and multiple-vehicle crashes, the base crash frequency for barrier-separated managed lanes is the lowest, followed by stripe-separated managed lanes and then pylon-separated managed lanes. This trend is shown graphically in Figure 25.

**Table 24. Calibrated Coefficients for Non-Reversible Managed Lanes.**

| Coefficient | Variable | Value | Std. Dev | *t*-statistic | *p*-value |
|---|---|---|---|---|---|
| $b_{sv,0}$ | Intercept, SV crashes, barrier buffer | −4.4765 | 1.7225 | −2.6 | 0.0096 |
| $b_{mv,0}$ | Intercept, MV crashes, barrier buffer | −5.5873 | 1.8356 | −3.04 | 0.0025 |
| $b_{sv,0}$ | Intercept, SV crashes, pylon buffer | −3.1353 | 1.6533 | −1.9 | 0.0585 |
| $b_{mv,0}$ | Intercept, MV crashes, pylon buffer | −4.797 | 1.7636 | −2.72 | 0.0068 |
| $b_{sv,0}$ | Intercept, SV crashes, striped buffer | −3.8811 | 1.5508 | −2.5 | 0.0126 |
| $b_{mv,0}$ | Intercept, MV crashes, striped buffer | −4.9585 | 1.6813 | −2.95 | 0.0033 |
| $b_{sv,1}$ | AADT, SV crashes | 0.4401 | 0.1685 | 2.61 | 0.0093 |
| $b_{mv,1}$ | AADT, MV crashes | 0.6055 | 0.181 | 3.35 | 0.0009 |
| $b_{is,sv}$ | Inside shoulder width, SV crashes | −0.01856 | 0.01512 | −1.23 | 0.22 |
| $b_{os,mv}$ | Outside shoulder width, MV crashes | −0.04018 | 0.02005 | −2 | 0.0456 |
| $b_{wev}$ | Access weaving section density | 0.2721 | 0.1164 | 2.34 | 0.0198 |
| $b_{ramp}$ | Access ramp gore density | 0.04173 | 0.02938 | 1.42 | 0.156 |
| $\delta_{sv}$ | Overdispersion parameter, SV crashes | 0.3039 | 0.1014 | 3 | 0.0029 |
| $\delta_{mv}$ | Overdispersion parameter, MV crashes | 0.4634 | 0.1054 | 4.4 | < 0.0001 |
| **Fit Statistics** | | | | | |
| Akaike's Information Criterion (AIC): 1404.2 | | Bayesian Information Criterion (BIC): 1463.5 | | | |
| Corrected Akaike's Information Criterion (AICC): 1405.0 | | −2 Log Likelihood: 1376.2 | | | |

**a. Single-Vehicle Crashes**　　　**b. Multiple-Vehicle Crashes**
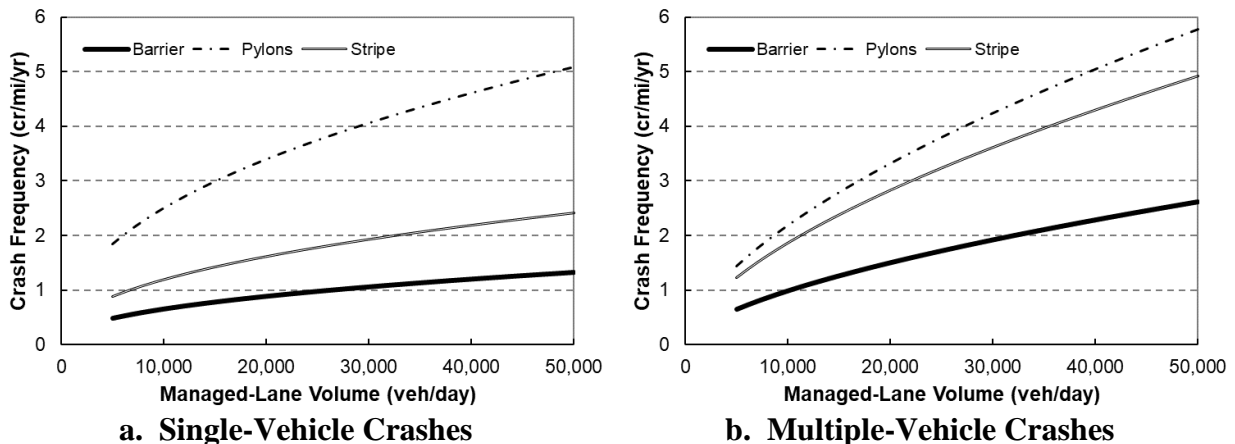
**Figure 25. Non-Reversible Managed Lane SPFs.**

Figure 26a illustrates the shoulder width CMFs. Inside and outside shoulder widths were found to have a similar effect on crash frequency, but with inside shoulder width affecting single-vehicle crashes and outside shoulder width affecting multiple-vehicle crashes.



**a. Shoulder Width**　　　**b. Access Point Density**
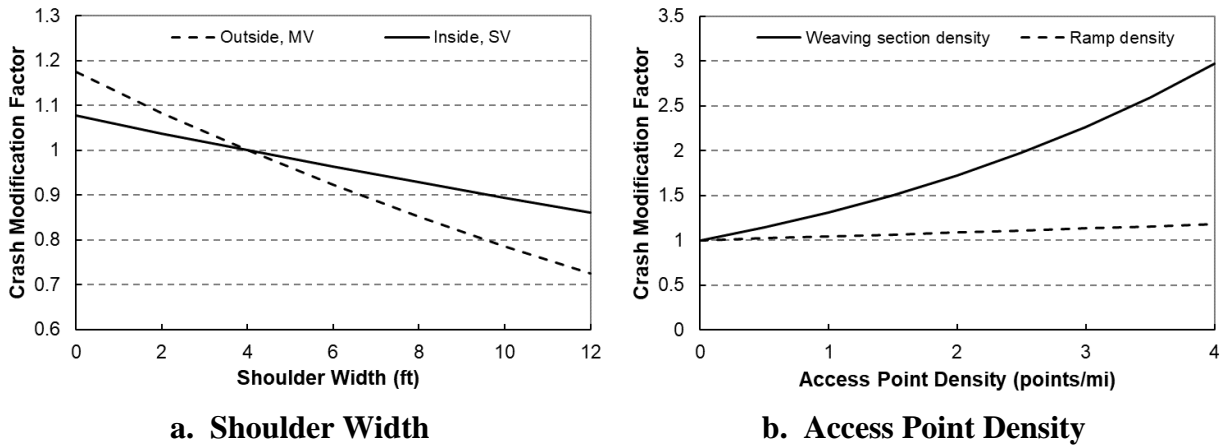
**Figure 26. Non-Reversible Managed Lane CMFs.**

Figure 26b illustrates the access point density CMFs. Both types of access points are shown to increase crash frequency, with higher CMF values for access weaving sections than for access ramp gores. The analysis did not show a difference in safety effects between the two types of access weaving sections (weaving in the general-purpose lanes or in the managed lanes as shown in Figure 15). The trends in these CMFs were affected by both access type and access point volume, the latter of which was not available to the research team. The selection of access type (i.e., weaving section versus ramp) was primarily affected by considerations of operations and geometry, particularly the origins and destinations of the managed-lane users.

The calibrated non-reversible managed lane SPFs for barrier buffers are described in equation form as follows:

$$N_{spf,sv} = L\,e^{-4.4765+0.4401\ln(AADT)} \tag{40}$$

$$N_{spf,mv} = L\,e^{-5.5873+0.6055\ln(AADT)} \tag{41}$$

The calibrated non-reversible managed lane SPFs for pylon buffers are described in equation form as follows:

$$N_{spf,sv} = L\,e^{-3.1353+0.4401\ln(AADT)} \tag{42}$$

$$N_{spf,mv} = L\,e^{-4.7970+0.6055\ln(AADT)} \tag{43}$$

The calibrated non-reversible managed lane SPFs for striped buffers are described in equation form as follows:

$$N_{spf,sv} = L\,e^{-3.8811+0.4401\ln(AADT)} \tag{44}$$

$$N_{spf,mv} = L\,e^{-4.9585+0.6055\ln(AADT)} \tag{45}$$

The CMFs for the non-reversible managed lane models are described in equation form as follows:

$$CMF_{is,sv} = e^{-0.01856(W_{is}-4)} \tag{46}$$

$$CMF_{os,mv} = e^{-0.04018(W_{os}-4)} \tag{47}$$

$$CMF_{wev} = e^{(0.2721[n_{wev}/L])} \tag{48}$$

$$CMF_{ramp} = e^{(0.04173[n_{ramp}/L])} \tag{49}$$

*Reversible Lanes*

Table 25 contains the calibrated coefficients for reversible managed lanes. The SPF coefficients $b_{sv,0}$, $b_{mv,0}$, $b_{sv,1}$, and $b_{mv,1}$ show that reversible-lane facilities with one lane will have more single-vehicle crashes but fewer multiple-vehicle crashes than facilities with two or more lanes. This trend is shown graphically in Figure 27. Note that the *y*-axis scales show that multiple-vehicle crashes are far more frequent than single-vehicle crashes on reversible managed-lane facilities.

Figure 28a illustrates the average shoulder width CMF for multiple-vehicle crashes on reversible managed-lane facilities. The trend of this CMF suggests that average shoulder width has a notable effect on multiple-vehicle crash frequency. Figure 28b illustrates the access ramp density CMF for reversible managed-lane facilities. The trend of this CMF shows an increase in crash frequency as access ramp density increases. This increase is similar in magnitude to the increase associated with access ramps on non-reversible facilities (see Figure 26b).

**Table 25. Calibrated Coefficients for Reversible Managed Lanes.**

| Coefficient | Variable | Value | Std. Dev | t-statistic | p-value |
|---|---|---|---|---|---|
| $b_{sv,0}$ | Intercept, SV crashes | −7.2209 | 2.3675 | −3.05 | 0.0024 |
| $b_{mv,0}$ | Intercept, MV crashes | −15.3049 | 3.0881 | −4.96 | < 0.0001 |
| $b_{sv,1}$ | AADT, SV crashes | 0.7047 | 0.2603 | 2.71 | 0.007 |
| $b_{mv,1}$ | AADT, MV crashes | 1.6653 | 0.3383 | 4.92 | < 0.0001 |
| $b_{nl,sv}$ | Number of lanes, SV crashes | 0.2782 | 0.2101 | 1.32 | 0.1862 |
| $b_{nl,mv}$ | Number of lanes, MV crashes | −0.7606 | 0.2621 | −2.9 | 0.0039 |
| $b_{s,mv}$ | Shoulder width, MV crashes | −0.3369 | 0.1043 | −3.23 | 0.0013 |
| $b_{ramp}$ | Access ramp density | 0.0503 | 0.03999 | 1.26 | 0.2091 |
| $\delta_{sv}$ | Overdispersion parameter, SV crashes | 0.3767 | 0.1515 | 2.49 | 0.0133 |
| $\delta_{mv}$ | Overdispersion parameter, MV crashes | 0.5512 | 0.1627 | 3.39 | 0.0008 |
| **Fit Statistics** | | | | | |
| Akaike's Information Criterion (AIC): 953.4 | | Bayesian Information Criterion (BIC): 994.5 | | | |
| Corrected Akaike's Information Criterion (AICC): 953.9 | | −2 Log Likelihood: 933.4 | | | |
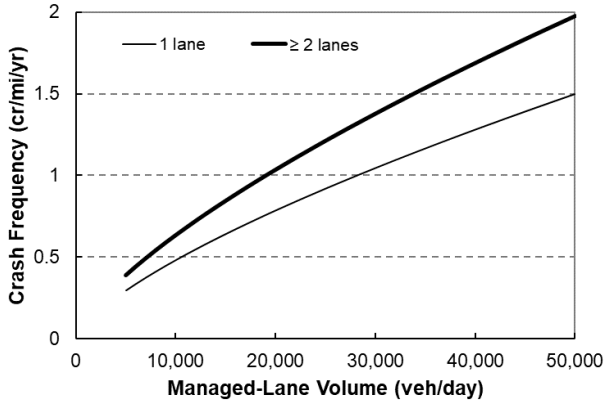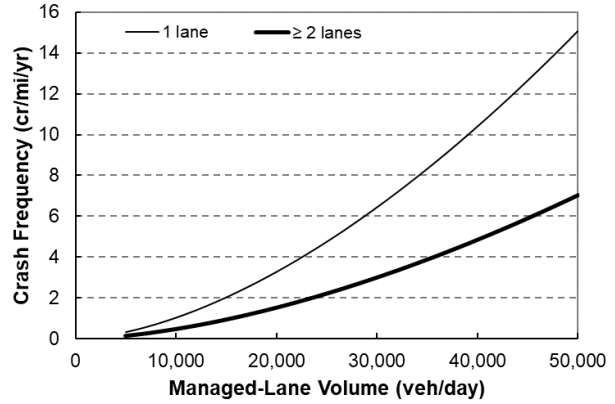


a. Single-Vehicle Crashes      b. Multiple-Vehicle Crashes

**Figure 27. Reversible Managed Lane SPFs.**



a. Shoulder Width (MV crashes)      b. Access Ramp Density

**Figure 28. Reversible Managed Lane CMFs.**

The calibrated reversible managed lane SPFs and CMFs are described in equation form as follows:

$$N_{spf,sv} = L\, e^{-7.2209+0.7047\ln(AADT)} \tag{50}$$

$$N_{spf,mv} = L\, e^{-15.3049+1.6653\ln(AADT)} \tag{51}$$

$$CMF_{nl,sv} = e^{0.2782 I_{nl}} \tag{52}$$

$$CMF_{nl,mv} = e^{-0.7606 I_{nl}} \tag{53}$$

$$CMF_{s,mv} = e^{-0.3369(W_s-2)} \tag{54}$$

$$CMF_{ramp} = e^{(0.0503[n_{ramp}/L])} \tag{55}$$

## APPLICATION

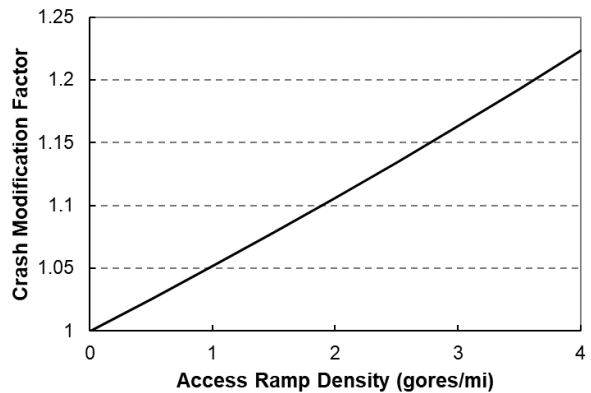### Using the Local Calibration Factors

Table 21 and Table 23, respectively, contain the local SPF and SDF calibration factors to be used with the HSM safety prediction models for urban freeways with 4–10 general-purpose lanes. The research team recommends pairing the calibration factors with the HSM models as shown in Table 26. Table 22 contains local calibration factors that can be used with the HSM 10-lane model to analyze urban freeway segments with 12 general-purpose lanes. These factors are provided in the bottom row of Table 26. The calibration factors can apply to the models for segments or speed-change lanes.

**Table 26. Summary of Recommended Local Calibration Factors for HSM Models.**

| Number of Lanes | HSM Model | Local SPF Calibration Factor by Crash Type and Severity | | | | Local SDF Calibration Factor |
|---|---|---|---|---|---|---|
| | | SV-FI | SV-PDO | MV-FI | MV-PDO | |
| 4 | 4 lanes | 0.77 | 0.68 | 0.65 | 0.57 | 2.18 |
| 6 | 6 lanes | 0.70 | 0.56 | 0.95 | 0.71 | 1.86 |
| 8 | 8 lanes | 1.25 | 1.04 | 1.27 | 1.20 | 1.64 |
| 10 | 10 lanes | 1.02 | 0.95 | 1.41 | 1.30 | 1.80 |
| 12 | 10 lanes | 1.01 | 0.77 | 1.13 | 1.04 | 1.80 |

The research team included some segments with odd-numbered lane counts in the calibration datasets but does not recommend directly applying the models to segments with odd-numbered lane counts. Instead, the research team recommends applying the HSM guidance for analyzing such segments. Specifically, if a segment has an odd number of lanes, $x$, it should be analyzed as if it had $x-1$ lanes and again as if it had $x+1$ lanes, and the predicted crash frequencies obtained from those two analyses should be averaged. This method can only be applied if the number of lanes in the two directions of travel differs by no more than one lane.

### Analyzing an Urban Freeway with Managed Lanes

The calibrated safety prediction models for managed lanes on urban freeways are described by Equations 40–55. These models, including their SPFs and accompanying CMFs, are summarized in Table 27. These models require the traffic volume for the managed lanes and apply to all crashes associated with the managed lanes, including crashes involving crossing

buffers or accessing the managed lanes (e.g., crashes in or associated with access weaving sections, whether the weaving sections are located in the managed lanes or in the general-purpose lanes, as shown in Figure 15). Safety performance in the adjacent general-purpose lanes is analyzed using the appropriate models and local calibration factors from Table 26. When applying the models for the general-purpose lanes, the managed-lane space in the median should be considered as non-traversable median space if a barrier or pylon buffer is present, or traversable median space if a stripe buffer is present.

**Table 27. Summary of Urban Freeway Managed-Lane Safety Prediction Models.**

| Facility Type | Crash Type | SPF Equation Number | CMF | CMF Base Condition | CMF Equation Number |
|---|---|---|---|---|---|
| Non-reversible, barrier-separated | SV | 40 | Inside shoulder width | 4 ft | 46 |
| | | | Access ramp | None present | 49 |
| | MV | 41 | Outside shoulder width | 4 ft | 47 |
| | | | Access weaving section | None present | 48 |
| | | | Access ramp | None present | 49 |
| Non-reversible, pylon-separated | SV | 42 | Inside shoulder width | 4 ft | 46 |
| | | | Access ramp | None present | 49 |
| | MV | 43 | Outside shoulder width | 4 ft | 47 |
| | | | Access weaving section | None present | 48 |
| | | | Access ramp | None present | 49 |
| Non-reversible, stripe-separated | SV | 44 | Inside shoulder width | 4 ft | 46 |
| | MV | 45 | Outside shoulder width | 4 ft | 47 |
| Reversible | SV | 50 | Number of lanes | 1 lane | 52 |
| | | | Access ramp | None present | 55 |
| | MV | 51 | Number of lanes | 1 lane | 53 |
| | | | Average shoulder width | 2 ft | 54 |
| | | | Access ramp | None present | 55 |

## Applying Empirical Bayes Adjustments

Table 28 contains the overdispersion parameters obtained from the model calibration efforts. These parameters can be used to apply the empirical Bayes method along with the calibrated safety prediction models to obtain estimated crash frequency.

**Table 28. Overdispersion Parameters for Empirical Bayes Applications.**

| Urban Freeway Facility Type | Overdispersion Parameter by Crash Type and Severity | | | | Source Table |
|---|---|---|---|---|---|
| | SV-FI | SV-PDO | MV-FI | MV-PDO | |
| General-purpose lanes, 4 lanes | 0.14 | 0.42 | 0.24 | 0.37 | Table 21 |
| General-purpose lanes, 6 lanes | 0.21 | 0.45 | 0.16 | 0.18 | |
| General-purpose lanes, 8 lanes | 0.10 | 0.11 | 0.09 | 0.07 | |
| General-purpose lanes, 10 lanes | 0.05 | 0.06 | 0.01 | 0.01 | |
| General-purpose lanes, 12 lanes | 0.09 | 0.03 | 0.02 | 0.01 | Table 22 |
| Managed lanes, non-reversible | 0.30 | | 0.46 | | Table 24 |
| Managed lanes, reversible | 0.38 | | 0.55 | | Table 25 |

# APPENDIX: VALUE OF RESEARCH ANALYSIS

## OVERVIEW

The research team conducted a value of research (VOR) analysis to produce an estimate of the benefit that the project will likely yield for TxDOT. The temporal scope for this analysis was an eleven-year period (labeled as years 0–10) starting with the beginning of the two-year project. The value of the project was described in terms of net present value (NPV) and cost-benefit ratio (CBR), which are computed using economic discounting formulas.

The primary objectives of TxDOT Research Project 0-7067 are to derive local calibration factors for the HSM models for urban freeways and to calibrate new safety prediction models for managed-lane facilities on urban freeways. Hence, the research team focused the VOR analysis on the safety benefits of widening urban freeways and barrier-separating managed lanes and the resulting cost savings that can be obtained by improving this safety knowledge.

## METHODOLOGY

The research team used a VOR template provided by TxDOT to compute the NPV and CBR measures. The template required the following items:

- Project budget: $275,000 ($92,141 in year 0, $155,797 in year 1, and $27,062 in year 2).
- Project duration: 2.5 years.
- Expected value duration: 10 years (convention chosen by TxDOT).
- Discount rate: 3 percent (default value assumed by TxDOT).
- Expected value per year: to be computed.

The project's expected value per year must be estimated based on a quantifiable analysis method that accounts for the benefit of the improved safety knowledge to be obtained through the research, as well as the number of curve sites expected to be treated and the cost of a pavement friction treatment. The analysis method is described in the following sections.

### Concept

An analysis method that can be used to estimate the benefit of conducting a research project on a safety treatment is documented in NCHRP Report 756 (*43*, *44*). The analysis method is summarized in the following paragraphs. This method is based on the following premise: there are numerous safety treatments available that can reduce crash frequency. Knowledge of the effectiveness of these treatments is typically expressed in terms of a CMF. Practitioners must apply CMFs to assess the potential effectiveness of a safety treatment before installing it in the field. To prioritize the many competing safety research project ideas (which yield new or improved CMFs), it is necessary to conduct a VOR analysis.

To conduct a VOR analysis, it is necessary to conduct the following steps:

1. Identify target sites where a treatment can be implemented.
2. Determine the distribution of target crashes for these sites.

3. Determine the mean and standard deviation of a CMF for the treatment (i.e., describe the certainty of the safety knowledge of the treatment) based on previous research.
4. Determine the expected standard deviation of the CMF (i.e., estimate the degree to which knowledge of the treatment's effectiveness can be improved) after the proposed new research project is completed.
5. Apply the procedure to estimate the expected value of the research.

For TxDOT Research Project 0-7067, the treatments of interest are widening urban freeways and barrier-separating managed-lane facilities that are currently stripe- or pylon-separated. Conducting this research project yielded improved knowledge of the base crash frequencies observed on the various types of urban freeways. This improved knowledge will reduce losses that TxDOT would otherwise incur by:

- Installing a treatment at a site where the treatment is not justified based solely on safety considerations.
- Failing to install a treatment at a site where the treatment is justified, thereby missing an opportunity to reduce the frequency and/or severity of crashes.

**Input Data**

The VOR analysis method documented in NCHRP Report 756 is implemented using a spreadsheet program called *Safety Research Prioritization Worksheet* (SRPW), which is available from NCHRP and described in a user manual (*45*). The required input data, values, and sources are listed in Table 29. The input data provide information about the candidate sites for treatment, safety knowledge of the treatment, crash cost, and treatment cost.

The research team queried the TRM database (see Table 4) to obtain an estimate of the total mileage of urban freeway segments in Texas by lane count. Based on the obtained distribution, the research team assumed that 50 miles of 8-lane urban freeway could be identified for widening to 10 lanes to improve safety performance, and another 50 miles of managed lanes with pylon or stripe buffer could have barrier buffers added to improve safety performance. The effect on safety performance for these two treatments was estimated as CMF values of 0.85 and 0.75, respectively, based on the SPF values for the facilities at their average AADT values of 250,000 veh/day and 20,000 veh/day, respectively.

To estimate the costs of crashes on rural highway curves, the research team chose 2021 as the analysis year and obtained the consumer price index (*46*) and employment cost index (*47*) values for that year. These values are 279 and 148, respectively. The research team queried the merged TRM-CRIS dataset used in the modeling efforts to obtain crash severity distributions and applied crash cost values from TxDOT's Highway Safety Improvement Program (HSIP) guidelines and National Safety Council estimates.

**Table 29. VOR Analysis Input Data and Sources.**

| Topic | Input Data | Value(s) | Source/Notes |
|---|---|---|---|
| Sites | Target highway miles | 50 | 8-lane freeway segments to have two lanes added |
| | | 50 | Pylon- or stripe-separated managed lanes to have barrier buffers added |
| | Average AADT, veh/day | 250,000 | Query of managed-lane volume data from operators |
| | | 20,000 | Query of TRM database |
| Safety knowledge | Mean CMF value (effect of countermeasure) | 0.85 | "Typical" value based on calibrated SPFs |
| | | 0.75 | |
| | Lowest and highest likely CMF values | 0.595, 1.148 | Used default assumptions of 70 percent and 135 percent of mean value for SRPW |
| | | 0.525, 1.013 | |
| Crash cost | Analysis year | 2021 | Assumed (most recent completed year) |
| | Consumer price index | 279 | US Department of Labor (*46*) |
| | Employment cost index | 148 | US Department of Labor (*47*) |
| | Crash distribution by severity | K = 0.006, A = 0.021, B = 0.105, C = 0.218, PDO = 0.650 | Query of merged TRM-CRIS database, 8-lane urban freeway segments |
| | | K = 0.009, A = 0.033, B = 0.187, C = 0.261, PDO = 0.510 | Query of merged TRM-CRIS database, non-reversible managed-lane segments |
| | Cost of K, A, B crash | $3.7 million, $3.7 million, and $520,000, respectively | TxDOT's HSIP guidelines (*48*) |
| | Costs of C and PDO crashes | $160,000, and $52,700, respectively | National Safety Council 2020 estimates (*49*) |
| Treatment cost | Treatment implementation level | All sites | Assumed |
| | Countermeasure service life | 25 years | Assumed |
| | Initial cost of project | $5,000,000/mi | Assumed based on similar construction projects |
| | | $1,000,000/mi | |
| | Annual maintenance cost of project | $0 per mile | Assumed no added maintenance cost due to treatment |

The research team assumed a service life of 25 years for both treatments and treatment costs of $5 million per mile and $1 million per mile, respectively, for the two treatments. The research team used an annual maintenance cost of $0 for analysis based on the assumption that maintenance costs would not increase following the installation of the treatments.

**RESULTS**

The research team conducted the VOR analysis using the SRPW program and obtained an annual VOR estimate of $237,154. This value represents the benefit that can be obtained if (1) the research project is conducted, (2) the results of the research project are used to analyze all relevant urban freeway segments that were identified in the TRM database query, and (3) the treatment is installed at all sites found to be "deserving" of treatment. A site is considered to

"deserve" treatment if the cost of treatment is less than the cost of the crashes that would be reduced over the service life of the treatment if the treatment were installed.

A summary of the VOR calculations is shown in Figure 29. The payback period for Research Project 0-7067 was found to be 1.16 years, and the cost-benefit ratio was found to be 5.38. These findings account for the construction costs and safety benefits incurred by TxDOT.

| | | Project # | 0-7067 | | |
|---|---|---|---|---|---|
| | | Project Name: | Enhancing Freeway Safety Prediction Models | | |
| | | Agency: | TTI | Project Budget | $ 275,000 |
| | | Project Duration (Yrs) | 2.5 | Exp. Value (per Yr) | $ 237,154 |
| | Expected Value Duration (Yrs) | | 10 | Discount Rate | 3% |
| Economic Value | | | | | |
| | Total Savings: | $ 1,676,527 | | Net Present Value (NPV): | $ 1,479,433 |
| | Payback Period (Yrs): | 1.16 | | Cost Benefit Ratio (CBR): | 5.38 |

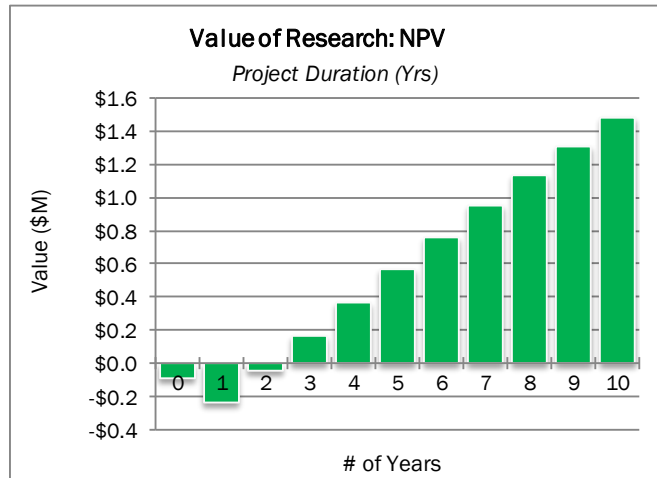| Years | Expected Value |
|---|---|
| 0 | -$92,141 |
| 1 | -$155,797 |
| 2 | $210,092 |
| 3 | $237,154 |
| 4 | $237,154 |
| 5 | $237,154 |
| 6 | $237,154 |
| 7 | $237,154 |
| 8 | $237,154 |
| 9 | $237,154 |
| 10 | $237,154 |



**Figure 29. VOR Analysis Results.**

# REFERENCES

1. Bonneson, J., and M. Pratt. *Roadway Safety Design Workbook.* Report No. FHWA/TX-09-0-4703-P2, Texas Transportation Institute, College Station, Texas, 2009.
2. *Highway Safety Manual.* American Association of State Highway Transportation Officials, Washington, DC, 2010.
3. Bonneson, J., S. Geedipally, M. Pratt, and D. Lord. Safety Prediction Methodology and Analysis Tool for Freeways and Interchanges, NCHRP Project No. 17-45. TRB, National Research Council, Washington, DC, 2012.
4. *Project Development Process Manual.* Texas Department of Transportation, Austin, Texas, 2017.
5. Dixon, K., K. Fitzpatrick, R. Avelar, M. Perez, S. Ranft, R. Stevens, S. Venglar, and T. Voigt. *Reducing Lane and Shoulder Width to Permit an Additional Lane on a Freeway.* Report No. FHWA/TX-15/0-6811-1, Texas A&M Transportation Institute, College Station, Texas, 2015.
6. Fitzpatrick, K., and R. Avelar. *Safety Implications of Managed Lane Cross Sectional Elements.* Report No. FHWA-HOP-10-076, Texas Transportation Institute, College Station, Texas, 2016.
7. Wunderlich, R., K. Dixon, L. Wu, S. Geedipally, B. Dadashova, and E. Shipp. *A Data-Driven Safety Analysis (DDSA) Framework for the Beaumont District.* Report No. 5-9052-01. Texas A&M Transportation Institute, College Station, Texas, 2019.
8. *Highway Capacity Manual.* Transportation Research Board, Washington, DC, 2010.
9. Council, F., and J. Stewart. Safety Effects of the Conversion of Rural Two-Lane to Four-Lane Roadways based on Cross-Sectional Models. *Transportation Research Record*, Vol. 1665, No. 1, 1999, pp. 35–43.
10. Milton, J., and F. Mannering. "The Relationship among Highway Geometrics, Traffic-Related Elements and Motor-Vehicle Accident Frequencies." In *Transportation*, Vol. 25, No. 4, 1998, pp. 395–413.
11. Noland, R., and L. Oh. "The Effect of Infrastructure and Demographic Change on Traffic-Related Fatalities and Crashes: A Case Study of Illinois County-Level Data." In *Accident Analysis & Prevention*, Vol. 36, No. 4, 2004, pp. 525–532.
12. Abdel-Aty, M., and A. Radwan. "Modeling Traffic Accident Occurrence and Involvement." In *Accident Analysis & Prevention*, Vol. 32, No. 5, 2000, pp. 633–642.
13. Kononov, J., B. Bailey, and B. Allery. Relationships between Safety and both Congestion and Number of Lanes on Urban Freeways. *Transportation Research Record*, Vol. 2083, No. 1, 2008, pp. 26–39.
14. Srinivasan, S., P. Haas, P. Alluri, A. Gan, and J. Bonneson. *Crash Prediction Method for Freeway Facilities with High Occupancy Vehicle (HOV) and High Occupancy Toll (HOT) Lanes.* Florida DOT Contract BDV32-977-04, University of Florida, Gainesville, Florida, 2015.
15. Moon, J., and J. Hummer. "Development of Safety Prediction Models for Influence Areas of Ramps in Freeways." In *Journal of Transportation Safety & Security*, Vol, 1, No. 1, 2009, pp. 1–17.
16. Hauer, E. *Observational Before-After Studies in Road Safety.* Emerald Publishing, Ltd., 2004.

17. Zheng, L., J. Sun, and X. Meng. "Crash Prediction Model for Basic Freeway Segments Incorporating Influence of Road Geometrics and Traffic Signs." In *Journal of Transportation Engineering, Part A: Systems*, Vol. 144, No. 7, 2018, pp. 176–189.

18. Haq, M., M. Zlatkovic, and K. Ksaibati. Freeway Truck Traffic Safety in Wyoming: Crash Characteristics and Prediction Models. *Transportation Research Record*, Vol. 2673, No. 10, 2019, pp. 333–342.

19. Dutta, N., and M. Fontaine. "Improving Freeway Segment Crash Prediction Models by Including Disaggregate Speed Data from Different Sources." In *Accident Analysis & Prevention*, Vol. 132.

20. Das, S., S. Geedipally, R. Avelar, L. Wu, K. Fitzpatrick, M. Banihashemi, M., and D. Lord. *Rural Speed Safety Project: Final Report*. Contract or Grant No. DTFH6116D00039L, 2020.

21. Hossain, M., and Y. Muromachi. "Development of a Real-Time Crash Prediction Model for Urban Expressway." In *Journal of the Eastern Asia Society for Transportation Studies*, Vol. 8, 2010, pp. 2092–2107.

22. Chen, R., M. Zhang, Z. Li, and W. Wang. "Development of Crash Prediction Model for Rear-End Collisions at Recurrent Bottlenecks on Freeways." In *CICTP 2012: Multimodal Transportation Systems—Convenient, Safe, Cost-Effective, Efficient*, 2012, pp. 2591–2602.

23. Xu, C., W. Wang, and P. Liu. "A Genetic Programming Model for Real-Time Crash Prediction on Freeways." In *IEEE Transactions on Intelligent Transportation Systems*, Vol 14, No. 2, 2012, pp. 574–586.

24. Ma, Z., H. Zhang, S. Chien, J. Wang, and C. Dong. "Predicting Expressway Crash Frequency using a Random Effect Negative Binomial Model: A Case Study in China." In *Accident Analysis & Prevention*, Vol. 98, 2017, pp. 214–222.

25. Roy, A., M. Hossain, and Y. Muromachi. Enhancing the Prediction Performance of Real-Time Crash Prediction Models: A Cell Transmission-Dynamic Bayesian Network Approach. *Transportation Research Record*, Vol. 2672, No. 38, 2018, pp. 58–68.

26. Yang, K., X. Wang, and R. Yu. "A Bayesian Dynamic Updating Approach for Urban Expressway Real-Time Crash Risk Evaluation." In *Transportation Research Part C: Emerging Technologies*, Vol. 96, 2018, pp. 192–207.

27. Sun, J., J. Sun, and P. Chen. Use of Support Vector Machine Models for Real-Time Prediction of Crash Risk on Urban Expressways. *Transportation Research Record*, Vol. 2432, No. 1, 2014, pp. 91–98.

28. Sun, J., and J. Sun. "A Dynamic Bayesian Network Model for Real-Time Crash Prediction using Traffic Speed Conditions Data." In *Transportation Research Part C: Emerging Technologies*, Vol. 54, 2015, pp. 176–186.

29. Sun, J., and J. Sun. "Real-time Crash Prediction on Urban Expressways: Identification of Key Variables and a Hybrid Support Vector Machine Model." In *IET Intelligent Transport Systems*, Vol. 10, No. 5, 2014, pp. 331–337.

30. Wang, G., and J. Kim. "A Large-Scale Neural Network Model for Real-Time Crash Prediction in Urban Road Networks." In *Compendium of the Transportation Research Board 97th Annual Meeting*, 2018.

31. Wang, X., Feng, M. "Freeway Single and Multi-Vehicle Crash Safety Analysis: Influencing Factors and Hotspots." Accident Analysis & Prevention, 132. In *Accident Analysis & Prevention*, Vol. 132, 2019.

32. Avelar, R. "A Workshop on Validation of Discrete Response Statistical Models." Presented at Conference for Statistical Practice, American Statistical Association, Portland, Oregon, 2018.

33. Lord, D., X. Qin, and S. Geedipally. *Highway Safety Analytics and Modeling*. Elsevier, 2021.

34. Washington, S., and W. Cheng. *High Risk Crash Analysis*. Report No. FHWA-AZ-05-558, University of Arizona, Tucson, Arizona, 2005.

35. Miaou, S. *Measuring the Goodness-of-Fit of Accident Prediction Models.* Publication No. FHWA-RD-96-040, U.S. Department of Transportation, Federal Highway Administration, McLean, Virginia, 1996.

36. Pilko, P., J. Bared, P. Edara, and T. Kim. *Safety Assessment of Interchange Spacing on Urban Freeways*. Publication No. FHWA-HRT-07-031, U.S. Department of Transportation, Federal Highway Administration, McLean, Virginia, 2007.

37. *Texas Manual on Uniform Traffic Control Devices*. Texas Department of Transportation, Austin, Texas, 2012.

38. *Houston Express Lanes Operations Summary*. Texas A&M Transportation Institute, College Station, Texas, December 2019.

39. Le, M., R. Macias, and S. Ranft. *Evaluation of TEXpress/Express Lanes: Draft Technical Memorandum*. Texas A&M Transportation Institute, College Station, Texas, December 2020.

40. Alluri, P., D. Saha, and A. Gan. "Minimum Sample Sizes for Estimating Reliable Highway Safety Manual (HSM) Calibration Factors." In *Journal of Transportation Safety & Security*, Vol. 8, No. 1, 2016, pp. 56–74.

41. Lyon, C., B. Persaud, and F. Gross. *The Calibrator: An SPF Calibration and Assessment Tool User Guide*. Report No. FHWA-SA-17-016. U.S. Department of Transportation, Washington, DC, 2016.

42. Cameron, A., and P. Trivedi. *Regression Analysis of Count Data*. Econometric Society Monograph No. 53, Cambridge University Press, 2013.

43. Zegeer, C., R. Srinivasan, D. Carter, F. Council, F. Gross, M. Sawyer, E. Hauer, J. Bonneson, and G. Bahar. *Highway Safety Research Agenda: Infrastructure and Operations*. NCHRP Report 756. TRB, National Research Council, Washington, DC, 2013.

44. Pratt, M., J. Bonneson, and C. Zegeer. Limiting Driveway Access at Intersections: Sample Application of Value-of-Research Evaluation. In *Transportation Research Record: Journal of the Transportation Research Board, No. 2432,* TRB, National Research Council, Washington, DC, 2014.

45. Zegeer, C., R. Srinivasan, D. Carter, F. Council, F. Gross, M. Sawyer, E. Hauer, J. Bonneson, and G. Bahar. *Highway Safety Research Agenda: Infrastructure and Operations*. NCHRP Report 756, Appendix G. http://onlinepubs.trb.org/onlinepubs/nchrp/docs/NCHRP17-48_Appendices.pdf. Accessed October 20, 2016.

46. Consumer Price Index. U.S. Department of Labor, Bureau of Labor Statistics. http://www.bls.gov/cpi/. Accessed May 31, 2022.

47. Employment Cost Index. U.S. Department of Labor, Bureau of Labor Statistics. http://www.bls.gov/news.release/eci.toc.htm. Accessed May 31, 2022.

48. *Highway Safety Improvement Program Guidelines*. Texas Department of Transportation, Austin, Texas, 2021.

49. Guide to Calculating Costs.  National Safety Council.  https://injuryfacts.nsc.org/all-injuries/costs/guide-to-calculating-costs/data-details/.  Accessed May 31, 2022.